The role of extracellular matrix composition and mechanical properties in driving cardiac differentiation of mesenchymal stem cells

A Thesis Submitted By

Joshua I N Resnikoff

In Partial Fulfillment of the Requirements for the Degree of

Master of Science

in

Biomedical Engineering

From

Tufts University

May 2012

Advisor: Lauren D Black, III

Abstract

Non-lethal myocardial infarction (MI) generates a scar within the myocardium that can result in long-term complications for the patient. Considerable effort has been directed toward cell-based therapies for cardiac repair and regeneration, but these approaches have been hampered by the non-proliferative nature of adult cardiomyocytes. To overcome this hurdle, a significant amount of research has been focused on generating cardiomyocytes from a proliferating pluripotent cell population. A number of successes have been achieved, but generally suffer from low rates of efficiency that obviate their use in clinical therapies. However, two areas of research show promise for promoting directed differentiation in pluripotent stem cells: 1) the use of decellularized extracellular matrix as a culture substrate and 2) the demonstration that substrate stiffness alone can direct differentiation. Our hypothesis was that using decellularized cardiac ECM to mimic the composition of the developing heart *in vitro* would promote cardiogenesis in mesenchymal stem cells (MSCs), and that this differentiation would be modulated by physiologically relevant stiffnesses. Rat MSCs were cultured on polyacrylamide gels of experimentally determined stiffness that incorporated rat cardiac ECM derived from specific life points. MSCs were interrogated for expression of the cardiac transcription markers Nkx2.5, GATA4, Tbx5, Mef2C, cTnI, and MHC at 1 and 3 weeks. MSCs cultured on neonatal ECM demonstrate the highest expression levels, and the expression is positively modulated by non-infarct-like stiffnesses. In addition, we began preliminary investigations into the role of integrin-binding peptide domains on cell signaling, as well as an exploration of alternate methods for solubilizing total ECM in order to generate a three dimensional hydrogel from it. This novel, soluble factor-free, cell culture platform advances the idea of ECM-mediated cell signaling and its ability to effect pluripotent stem cell differentiation.

Acknowledgements

I would like to thank my advisor, Dr Lauren Black III, for his guidance and support throughout this work. I would also like to thank Dr Gordon Huggins for serving on my thesis committee; Dr David Kaplan deserves heart-felt thanks for all of his encouragement and support during my time at Tufts. I could not have accomplished my work without the help of my lab mates Dr Corin Williams, Kathy Ye, Kelly Sullivan, and Rachel Twardowski, nor without the assistance of my undergraduates Katherine Tang, Rushab Shah, and David Sutherland. My Parents continue to be an amazing source of wisdom, and I doubt if I could accomplish much without the love, support, and [bottomless] patience of my wife, Christine. Thank you everyone!

Table of Contents

List of Table

List of Figures

1. Introduction

The goal of this research was to develop a novel cell culture platform with defined mechanical and compositional properties. More particularly, the platform was focused on mimicking the environment associated with cardiac development in an effort to drive bone-marrow mesenchymal stem cells (MSC) toward cardiomyocyte differentiation. The ability to induce differentiation of MSCs toward a variety of outcomes by stiffness or substrate composition has been previously demonstrated (13, 15, 24, 30, 41, 54, 74, 80, 83). However the efficiency of promoting cardiac differentiation of MSCs without the addition of soluble factors has remained too low for therapeutic application. This thesis describes the development of, and experimentation with, a novel approach for recreating the developmental environment of cardiac tissue by incorporating solubilized cardiac extracellular matrix (ECM) of specific developmental ages into a polyacrylamide hydrogel. In addition, concurrent experiments exploring alternate ECM solubilization methods and means for reliably forming a hydrogel from solubilized ECM are described.

Chapter 2 will frame this research by starting with an examination of the current

clinical gaps in applied cell-based engineering. Next, an overview of the cardiac development pathway will be given, followed by a review of the role of the extracellular matrix and integrin-mediated signaling in cardiac differentiation. Finally current and previous research in controlling stem cell differentiation will be discussed, forming the background for the development of our hypothesis and approach of cardiac differentiation of MSCs without soluble factors.

Chapter 3 provides the bulk of the thesis work, describing every step of the process of developing our new platform and interrogating its ability to aid in cardiac differentiation of MSCs. This chapter is comprised of three main sub-chapters: the first part outlines the methods and developed protocols for isolating rat cardiac ECM and our characterization of its mechanical properties and composition; the second part focuses on the development of the polyacrylamide hydrogel platform and assessing its ability to support MSC adherence and proliferation; the final section outlines our experimental design for using the platform for cardiac differentiation, and reports our data related to this goal. The chapter ends with conclusions regarding our findings and comments on future application.

Chapter 4 highlights work undertaken in a collaborative effort with Dr Qiaobing Xu's group to gain insight into specific cell-signaling mechanisms related to integrin-binding events. Integrin binding peptides of interest were purchased and functionalized to a gold surface sputtered onto a glass slide, onto which MSC were cultured and observed. This chapter describes the methods and reports on our preliminary data thus far.

Chapter 5 outlines our investigations into alternate methods for solubilizing ECM. Currently, the commonly accepted method utilizes strong proteases to digest the ECM until it becomes a solution. Our work has attempted to achieve solubilization through alternate – and possibly less destructive – methods that have the potential to aid in the ability of the solubilized ECM to reform into a hydrogel. This chapter reviews the rationale for these approaches and our results to date.

Chapter 6 draws conclusions from the research, commenting on areas of

possible experimental error and the potential future investigations.

2. Background

2.1 Clinical Need

Myocardial infarction (MI) is the leading cause of death in the United States. Over 800,000 patients will suffer MI this year (1), resulting in a need for corrective surgery or eventual whole organ transplantation. MI is caused by the blockage of a cardiac artery that results in a decreased –or lack of - flow of oxygen and nutrients to cells downstream from the occlusion. The size and location of the blockage determines the volume of cardiac muscle affected and the onset speed of detrimental effects. Severe cases cause localized cell death, resulting in the formation of a scar (infarct) that impedes normal heart function (2).

The primary treatment for MI is the placing of a stent within the occluded artery to reperfuse it, a surgical process called angioplasty. In severe cases, where a stent or balloon angioplasty is not recommended either due to complications with restenosis (3, 6), the potential for repeated reperfusion (4), or total arterial obstruction (6), a cardiac bypass might be necessary. A bypass uses an autologous vessel (common sources include the thoracic arteries, saphenous veins, and radial arteries) to circumvent the blockage (5). Both of

these procedures are focused on reforming the cardiac vascular network to resupply the tissue downstream of the occlusion with nutrients, mitigating further negative effects. While these surgeries do provide improved life-expectancies for the patient (6), neither address the long-term complications associated with MI. The scar impedes normal electrical conduction through the myocardium (7, 8), which can lead to arrhythmia (7). The scar forms a dense, hypoxic environment that is not easily reorganized by natural wound-healing processes (10). To compensate for the decrease in function due to the loss of a portion of the cardiac muscle, the remaining healthy myocardium can undergo pathological cardiac hypertrophy (9), leading to ventricular dilation and loss of contractile function (93).

One method to restore function to the infarct is to suture over, or surgically replace, the dead tissue with a “heart patch”. The use of a patch to repair cardiac defects in the pericardium (18), aorta (20), and tetralogy of Fallot (19) go back over 40 years. A “heart patch” for use in the ventricular wall would be produced *in vitro*, and could be composed of cells alone (21) or a composite of cells within a scaffold (22). Promising results utilizing multicellular coculture and the suspension of cells within a scaffold for recapitulating cardiac function have been demonstrated in animals (21, 15), but have yet to attain human

application.

Cell-based therapies are an alternate approach that rely on injection of stem cells directly into the infarct, with (26) or without (25) a supporting adjuvant. Initially this approach resulted in improved cardiac output, but over time cardiac function returned to a diminished state due to low engraftment efficiency (as the cells died or migrated away from the injection site) (27). Alternate approaches utilizing skeletal myocytes also failed to sustain improved cardiac output over time due to lack of transdifferentiation of the cells into cardiomyocytes (27).

The above approaches share a commonality of generating cardiomyocytes to recapitulate heart function. While some cells of interest expand well *in vitro* from primary isolation (14), mature cardiomyocytes (CM) are terminally differentiated and maintain an extremely limited proliferative ability (27). This obviates the use of autologous CMs in therapeutic regenerative platforms. Standard methods for conducting CM primary isolation are unable to separate cardiac precursor cells (113), adding to the difficulty of expanding these cells to clinically relevant numbers. These hurdles have prompted exploration for an alternate source of patient-specific multipotent proliferating cells that can be

efficiently differentiated into cardiac muscle cells.

2.2 Cell Source Determines Clinical Applicability

There are a variety of cell sources that have the potential to provide a good option for generating cardiomyocytes. Cells that can differentiate into multiple tissues are generally referred to as –potent cells, prefixed with toti-, pluri-, or multi-. These designations roughly refer to how many tissue lineages can be attained by the cell. Totipotent cells can develop into any tissue within the body, pluripotent cells can form multiple tissues, and multipotent cells differentiate into multiple types of cells found within the same tissue.

Embryonic stem cells (ESC) are totipotent cells harvested from the inner layer of the blastocyst (28). They are highly expandable *in vitro* and have been previously shown to differentiate to functional cardiomyocytes *in vitro* when cultured with ascorbic acid (30), or cultured with other described differentiation media (29, 27). Autologous ESC will decrease the chances of a host-graft rejection (29), but this requires parental foresight to address a potential need, and the means to store them until that need is warrant. Current ongoing clinical

trials use allogeneic ESCs to treat spinal injury (114), but this risks an undesirable immune response and/or uncontrollable hypertrophy (29). Another considerable drawback for considering ESC in a regenerative medicine platform is their propensity *in vivo* to spontaneously develop benign and malignant polyclonal tumors (teratomas and teratocarcinomas, respectively) (31). The inability to control for complete and stable differentiation of the cells upon *in vivo* transplantation severely limits their current therapeutic potential.

Induced pluripotent stem cells (iPS) are a relatively new class of embryonic-like stem cells. They are derived by reactivating embryonic transcriptional factors in somatic cells, and can be achieved with any cell line from patients of all ages, including 69 year old male cheek epithelium (33), circumventing the need for foresight and long-term storage of ESC. Initial reporting required the overexpression of embryonic genes c-Myc, Klf4, Nanog, and Sox2 (94). Unfortunately c-Myc has been identified as an oncogene, and utilizing it in embryonic de-differentiation can result in high tumorgenicity when injected *in vivo* (34). Subsequent methods were capable of producing iPS without activating c-Myc and therefore with diminished tumor incidence, albeit through a much longer and less efficient process (34). These methods focused primarily on activation of Oct4 and Sox2 via retroviral or lentiviral infection (32, 33).

However, due to the random insertion of the embryonic genes within the genome by the viral vector, there is no way to guarantee that long-term complications won't arise. In fact, a recent study demonstrated a rejection of autologous re-programmed iPS cells in mice, attributed to epigenetic disturbances from the reprogramming process that culminated in increased T cell sensitivity (35, 36). This, and potential other challenges, highlight the difficulties using this cell type as a platform for transplantation therapies at this time.

Mesenchymal stem cell (MSC) refers to a population of adult pluripotent cells that demonstrate self-renewal (37). Large reservoirs can be found in the bone marrow (44) and adipose tissue (43). These cells have successfully been differentiated into a variety of tissue, including cartilage (39), bone (40, 41), fat (41), and skeletal muscle (42). Despite research citing a low efficiency of cardiomyogenic differentiation (50), MSCs have demonstrated cardiogenic potential and maturation when treated with the demethylating chemotherapeutic 5-azacytidine (45), or when co-cultured with native cardiomyocytes (49). Bone marrow provides a readily accessible reservoir of MSC that can be easily isolated and purified (46). This sub-population of MSC can be identified by their expression of CD13, CD44, CD73, CD90, CD105, CD166, and

STRO-1, and differentiated from alternate sources by their lack of CD14, CD34, and CD45 (47). Furthermore, MSC have been shown to utilize paracrine signaling to modulate host inflammation and suppress host immune response (48), decreasing the likelihood of implant rejection.

2.3 Markers of Cardiomyocyte Maturation

There are multiple unique transcription factors that can be readily identified during different stages of cardiac development. Nkx2.5 and GATA4 are commonly used as indicators of early cardiac induction of pluripotent stem cells, followed by commitment transcripts of Tbx5 and Mef2C. Cardiomyocyte maturation can be confirmed by the presence of connexin-43, myosin heavy chain, a-actin, and expression of cardiac-specific troponins.

Nkx2.5 is a member of the NK homeobox family, a cardiac-specific gene conserved across species (108). It is one of the earliest transcription factors to be easily detected during cardiogenesis (107). Likewise, GATA4 is a cardiac-tissue specific marker for pre-cardiac cells. It is a zinc-finger transcription factor that, through physical interaction with Nkx2.5, synergistically upregulates

downstream cardiogenic commitment transcription (106).

Two cardiac commitment transcription factors are Tbx5 and Mef2C. Nkx2.5 and Tbx5 both directly bind to the promoter region for cardiac-specific natriuetic peptide precursor A (Nppa) (108); Tbx5 is part of the t-box transcription factors, known to play key roles in organ development. Myocyte enhancer factor 2, polypeptide C (Mef2C) belong to the conserved homeobox MADS-box family, and is essential for expression of cardiac muscle genes. Mef2C is downregulated by deficient Nkx2.5 and/or GATA4 expression, but contains GATA binding sites; overexpression of Mef2C can induce both Nkx2.5 and GATA4 expression and lead to cardiomyogenesis in P19 cells (110). Although the temporal hierarchy is unclear, it appears to act as a positive regulatory loop that supports and maintains cardiomyogenesis (109).

Mature cardiomyocytes are identified by their expression of the proteins myosin, α-actin, and troponins, which form the organized functional unit that generates force within the cell. The actin (thin) filament is a double helix with staggered active sites that allow the myosin to form cross-bridges, ratcheting the end-plate z-disks toward each other during muscle contraction (also called sliding filament mechanism). Myosin (thick filament) has two heavy chains that

form a double helix “tail” that splits bilaterally to form the myosin “head” with the additional light chains (2). The troponins form molecular complexes (with topomyosin) that inhibit the natural-binding of the myosin head to the actin active sites. Although the exact mechanism is unclear, it is known that Ca ions bind troponin C, which alters the troponin complex and uncovers the active site to initiate contraction (2).

2.4 Extracellular Matrix Roles in Attachment and Signaling

Organs and tissues are not made of cells alone. The interstitial matrix and basement membrane have long been identified as key components of organ structure and function. However, it was previously believed that this function was to act as merely a static support for cellular attachment, organizing the cells in space so that they could properly function. This view has changed in recent years. It is now generally accepted that the extracellular matrix (ECM) is a dynamic, complex organization of proteins, polysaccharides, and glycoproteins, simultaneously altered by the cells that it serves as a structural support replete with signaling moieties (51).

The protein fraction of ECM is composed primarily of the macromolecules collagen, laminin, elastin, and fibronectin. These proteins are constitutive throughout the body, but are expressed in varying ratios dependent upon tissue location, form, and function. Further proteomic analysis has identified hundreds of additional proteins associated with the ECM, both constitutively and transiently expressed (57). Some of them, like periostin, are known to change in concentration over time and have been postulated as regulator of cardiac development (56).

Collagen is the most abundant ECM protein in the body, comprising 25 – 35% of total protein. Collagen is a right handed coiled coil comprised of 3 α chain left-handed helix polypeptides. The α chains are built from repeating amino acid sequences of either Glycine-Proline-x, or Glycine-x-Hydroxyproline, wherein x is a different amino acid. The coiled coils (microfibrils) associate with other coiled coils to become a super-coil (fibril). Over 30 distinct collagen fibrils have been identified (95), and their unique peptide sequences have been implicated in specific tissue associations (78). Collagen I is the most ubiquitous amongst mammalian tissues, primarily aiding in tensile (96). The other main isoforms of collagen have noted expression in cartilage (Type II) (98), developing tissues alongside type I (Type III) (97), association with the basement membrane and

fibronectin (Type IV) (99), and in matrix assembly (Type V) (100). Cells express at least 8 different types of collagen binding receptors, 4 of which have been identified as integrins (57).

Laminin is a heterotrimeric protein comprised of an alpha, beta, and gamma subunit. There are 15 identified isoforms denoted by the 3 digit code representing each respective subunit (ie: α2, β1, γ1 corresponds to LAM211 protein). The peptide chains form a cross structure, wherein the alpha chain forms the central support with the smaller beta and gamma chains branching off opposing sides. This conformation allows laminin to bind together to form interconnected laminin sheets, which accounts for the majority of the basal lamina (basement membrane), and to bind alternate ECM proteins (collagen IV and fibronectin) and cell-surface receptors. Laminin is known to be important in integrin-mediated binding events by reorganizing the cytoskeleton, and knockouts have demonstrated lethality (53). Furthermore, it has been shown to promote neural differentiation and provide a stable proliferative environment for human ESC and iPS without additional support (54).

Elastin is the primary component of elasticity within the body. The precursor tropoelastin is theorized to be deposited onto a fibrillin microfibrillar

template (52). It is composed of helical regions of hydrophobic polypeptides (rich in glycine) with linear chains of lysine residues (52). The elastin is cross-linked by lysal oxidase at these lyseine regions, allowing the coiled portions to deforming under load and recoiling to its original shape (115). This insoluble web is responsible for a critical mechanical function, but little is known about how elastic fibers regulate cell behavior (52).

There are two types of fibronectin found within the body: one is secreted by the hepatocytes and is found as a soluble form within the blood plasma, the other is an insoluble component of the ECM (this latter form will be referred to herein). The protein is a near homologous dimer built from monomers of three distinct modules (I, II, III) joined at the c-terminus (101). Modules I and II contain disulfide bonds and are known to bind other ECM proteins and fibronectin "assembly" regions (101). Module III does not contain disulfide bonds (leading to alterations in access to its binding domains via tension (101)), but does contain binding regions for proteoglycans known to influence mitogenic processes (101). Additionally, there may or may not be a "V" region following module III that can be of varying length, but is known to bind VCAM-1 (101). Several integrin binding peptide sequences within the fibronectin protein sequence have been identified, including the attachment sequence RGD (III9) (58) and its synergy site PHSRN

(III10) (70). These regions are critical for successful wound healing (59), implicating the importance of fibronectin in ECM signal transduction.

2.5 The Role of Integrins in Cell Signaling

Individually the ECM proteins represent discrete binding and signaling sites that have been identified for their mitogenic effects (51-58). With recognition that different tissues, and different developmental timepoints, have different ratios of the ECM proteins, this would lead to tissue - and developmental age -specific binding domain patterns that could affect cell differentiation and maturation in a spatiotemporal manner. Thus the ECM exerts mitogenic influence over cellular differentiation and maturation. The key cell receptors that “read” these patterns are the integrins.

Integrins are transmembrane obligate heterodimer proteins composed of an alpha and beta subunit that are non-covalently associated. There are 18 alpha subunit isoforms and 8 beta subunit isoforms, however, only 24 paired heterodimers have been identified (102). Some integrins can be separated into three major families based on their beta subunit: cytoadhesion receptors (beta3)

(104), leukocyte adhesion receptors (beta2) (103), and very-late-antigen receptors (beta1) (103).

Although the exact mechanisms governing ECM signaling remain under investigation, it is known that the integrin's extracellular portion interacts with binding ligands in the extracellular matrix. This conveys tension through a site of focal adhesion (FA) that connects the ECM with the cytoskeleton a-actin via the intracellular proteins paxillin, talin, vinculin, VASP, zyxin, and a-actinin (89, 90). Recruitment of multiple integrins induces activation of their cytoplasmic domain to phosphoryle (activate) focal adhesion kinase (FAK) (91). FAK has been shown to influence mitogenic response through interaction in the MEK/ERK (86), Rac/Ras (88), Rho/Rock (85), and PI3 (87) pathways. Furthermore, integrin-mediated signaling is bi-directional, meaning that information is conveyed intra-to-extracellularly, allowing the cell to communicate information about itself to the outside environment (76). This is particularly useful to initiate an immune response, when integrins are expressed that bind complement (105).

2.6 Significance

It has been previously established that pluripotent cells respond to their local microenvironment as a function of substrate stiffness or composition. Specifically, Engler et al were able to direct MSC differentiation toward osteogenic, myogenic, and neurogenic lineages as a function of the cell culture substrate elasticity (15). Other studies have explored the cardiac differentiation potential of specific ECM proteins on MSC (13). But these microenvironmental features are not independent *in vivo*. Cardiac ECM is a complex mix of structural proteins with various local stiffnesses that change in a dynamic process over an individual's lifetime. As described above, these external cues are transmitted to the cell via integrin-ligand binding and associated tension fibers of the cytoskeleton that form specific focal adhesion sites. Multiple proteins are bound to cell receptors at the same time, producing an integrated response within the cell.

There is a wealth of research investigating the ability of pluripotent cells to differentiate into functional cardiomyocytes *in vitro* and *in vivo*. *In vitro* studies have promoted cardiopoeitic maturation through treatments with 5-azacytadine (60, 66), bone morphogenic protein (BMP-4) (61), fibroblast growth factor (FGF) (62), hepatocyte growth factor (HGF) (64), and hypoxic conditions (65). Some of these methods have been carried *in vivo* by injecting cells into an

MI model via the peripheral blood, coronary arteries, or into the MI scar directly (67). Unfortunately these methods have not demonstrated the desired success in terms of local engraftment (27). Chemical treatment yields low differentiation rates of <1% (66), and studies confirm that >90% of injected cells are not retained (27, 68). It has been suggested that preconditioning transplanted cells might increase treatment efficacy (27).

Pluripotent stem cell response to substrate stiffness is mediated through mechanotransduction. At its core, mechanotransduction is the process of translating mechanical stimuli into biological response inside the cell. It drives mechanotaxis (69), influences cellular tensegrity by acting directly on the cytoskeleton (69), and can influence binding-mediated signal transduction. For example, it has been demonstrated that tension is required for activation of integrin $\alpha 5\beta 1$ to bind the fibronectin synergy site, necessary for phosphorylation of FAK (70). Multiple studies have demonstrated the effects of stiffness on mitogenic processes like proliferation and differentiation in stem and differentiated cells (15, 71-75). Integrins have specifically been identified as key mediators in this process as part of “outside-in” signaling determined by substrate stiffness and topography, ligand density, and tissue deformation (76).

It is generally accepted that protein modification of a surface promotes a cellular response. Denatured collagen (gelatin) is commonly adsorbed to a surface to promote cell adhesion (81); adsorbed laminin has demonstrated influence over neural development and guidance (82). Other research has immobilized specific peptides to exploit their unique properties. The cytoadhesion domain RGD is recognized by more than half of known integrins (78), and is commonly used to promote cell attachment, and/or drive attachment of a deliverable like a drug-carrying nanoparticle (77). More specific integrin interactions have been identified: collagen I contains the GFOGER (glycine-phenylalanine-hydroxyproline-glycine-glutamic acid-arginine) peptide (with or without flanking GPP) that binds the $\alpha 2\beta 1$ integrin (80). Other peptides, like KRSR (lysine-arginine-serine-arginine) and FHRRIKA (phenylalanine- histidine-arginine- arginine- isoleucine- lysine- alanine), have been shown to interact with transmembrane proteoglycans and are critical components for osteogenic signaling (79).

In vivo the above factors are concomitant, but to date there has been limited research exploring pluripotent stem cell response to their coupled effects. Some work has functionalized single ECM proteins onto molded posts (83) or surfaces (13); alternate studies have examined the effect of culturing cells

on the complete ECM (16, 84). To gain more insight into the integrin-mediated mechanical and peptide signaling, a better mimic is required.

2.7 Moving Forward

Taken together, this background outlines the rationale for coupling the *in vivo* domains related to stiffness and total ECM signaling and probing their effect on cardiogenic induction. This thesis details our results concerning the novel two-dimensional platform of polyacrylamide and total ECM, preliminary results pertaining to peptide-linked mechanistic studies, and the attempts to produce a three-dimensional ECM hydrogel for future work geared toward the ultimate goal of an *ex vivo* platform for an increased efficiency of MSC cardiogenesis, modeling MI, and probing peptide-binding signaling mechanisms.

3. Investigation into the Mechanochemical Signaling Effects of Extracellular Matrix Proteins Coupled with Physiologically Relevant Mechanical Stiffness on Early Cardiac Differentiation of Mesenchymal Stem Cells

3.1 Introduction

This year, over 800,000 patients will suffer a myocardial infarction (MI) (1). The cell death induced by a blocked artery will result in the formation of a scar (infarct) that will impede normal heart function (2). The current gold standard treatment is a balloon angioplasty, with or without the implantation of a stent, to re-open the occluded artery and reperfuse the organ with blood. While this minimally-invasive surgery does improve patient life-expectancies (6), it does not address the long-term complications associated with MI. The infarct forms an ECM-dense, hypoxic environment that impedes normal electrical conduction through the myocardium (7, 8), can lead to arrhythmia (7), and is not easily reorganized (10). Over time, because it cannot be easily repopulated with cardiomyocytes, it can lead to pathological cardiac hypertrophy in the undamaged regions of the heart (9), causing ventricular dilation and overall loss of contractility (93).

To combat these complications, cell-based approaches are being developed that aim to supplement or recapitulate normal heart function through

therapeutic stem cell injection (25, 26) or the application of a cell-based cardiac patch (21-24), respectively. These efforts rely on generating cardiomyocytes to restore contractility within the heart. Unfortunately, mature cardiomyocytes that can be derived from the patient are terminally differentiated and maintain an extremely limited proliferate ability (27), obviating their expansion *in vitro*. This significant hurdle has prompted exploration for an alternate source of patient-specific pluripotent proliferating cells that can be efficiently differentiated into cardiac muscle cells (11-14, 17).

There are three common options for pluripotent cells that can be used for clinical therapy in the heart: embryonic stem cells (ESC), induced pluripotent stem cells (IPS) and mesenchymal stem cells (MSC). Complications with immune rejection (29), uncontrolled hypertrophy (29), teratoma formation (31), and inefficient activation (34) continue to hamper current cell therapies utilizing ESC and IPS. However, MSC are a population of autologous pluripotent cells that demonstrate self-renewal (37) and can be found in significant quantity in adult patients in the "reservoirs" of bone marrow (44) and adipose (43). They can be easily isolated and purified (46), and have been shown to modulate inflammation and the immune response (48). Furthermore, there is a wealth of research investigating the ability of MSC to differentiate into functional

cardiomyocytes *in vitro* (12-13, 16-17, 60-65) and *in vivo* (14, 22-26). *In vitro* studies have promoted cardiogenic maturation through treatments with 5-azacytadine (60, 66), bone morphogenic protein (BMP-4) (61), fibroblast growth factor (FGF) (62), hepatocyte growth factor (HGF) (64), and hypoxic conditions (65), but these can yield low differentiation rates of <1% (66), or use demethylating chemotherapeutic agents that could lead to a downstream lack of genetic control (e.g., 5-azacytidine). MSC cardiogenesis has also been demonstrated by co-culture with a high ratio of neonatal cardiomyocytes (49), but human neonatal cardiomyocytes are not readily available. Taken together, these current approaches demonstrate a low efficiency for inducing cardiac differentiation in MSC.

Recently Engler et al were able to direct MSC differentiation toward osteogenic, myogenic, and neurogenic lineages as a function of only the elasticity of the substrate on which the cells were seeded (15). Moreover, Tan et al demonstrated that plating Cardiac-Like Cells on Collagen V resulted in enhanced cardiac differentiation as compared to Collagen I (13). In both of these cases, the differentiation was attributed to signaling via integrin-mediated mechanotransduction pathways. Integrins are transmembrane heterodimeric proteins composed of paired alpha and beta subunits. They recognize and bind

to specific peptide sequences found within the proteins of the extracellular matrix (ECM), which is primarily composed of collagen, fibronectin, laminin, and elastin. Although there are many studies investigating the effects of these singular proteins on cell fate and function (59, 76, 101), these experiments do not accurately reflect the native environment. The integrins interact with the local ECM in its totality; to recapitulate that environment, total ECM must be utilized. Singular protein presentation might demonstrate an increased proliferation on collagen I (139), or an increased cell adhesion, but decreased proliferation, on fibronectin (81), but these studies fail to explain how the binding to these two proteins at the same time might synergistically or antagonistically affect the cell. Furthermore, while decellularized ECM has been shown to support cardiomyocyte function (23, 24), and substrate stiffness has been identified as important for cell function (15, 133), there is minimal published data exploring the combination of these factors and their potential role on MSC cardiac differentiation.

In the present study we hypothesized that using decellularized cardiac ECM to mimic the composition of the developing heart *in vitro* would promote cardiogenesis in MSCs, and that this differentiation would be modulated by physiologically relevant stiffnesses. We investigated the combined effects of

substrate stiffness and ECM composition via a polyacrylamide gel system that incorporated solubilized cardiac ECM into gels of physiologically relevant stiffnesses. In doing so, we are potentially able to decouple the effects of these environmental cues in order to assess whether the induction of cardiac transcription factors is derived from stiffness or composition (or some synergistic combination thereof), and therefore possibly implicate which is of greater importance to cell differentiation. To evaluate the effects of the stiffness-ECM combinations, we cultured MSCs for up to 3 weeks and assessed expression of known cardiac transcription and maturation markers by immunohistochemical staining and Western blot analyses. We further compared these results to MSCs grown on total ECM from an alternate organ source to evaluate the specificity of transcript activation. The results demonstrate a dynamic signaling environment that generates the strongest cardiac marker expression at physiologically coupled stiffnesses and ECM compositions from earlier developmental life stages.

3.2 Methods

3.2.1 Characterization of Rat Heart Extracellular Matrix

3.2.1.1 Heart Isolation

Hearts were isolated from Sprague-Dawley rats in accordance with our Tufts University IACUC approved protocol. Adult rats were euthanized by CO_2 asphyxiation prior to perforation of the diaphragm. To remove the heart, a median sternotomy was performed followed by the complete removal of the rib cage to grant unhindered access to the aorta. The heart was cleaned by gross dissection of the pericardium, thyroid and fat, followed by disruption of the local connective tissue. The aortic arch was cleaned of connective tissue in a similar fashion, allowing access to the first three arterial branch points. A 6-0 nylon suture (Ethicon) was used to ligate each of these branches. After all three branches were secured, the descending aorta was tracked behind the heart and cut approximately 0.5cm below the peak of the arch. The three arterial branches were trimmed distal to the sutures as the aorta was pulled away from the abdominal cavity. Next the vena cava and the pulmonary connections were removed and the entire heart-aorta system was transferred into 1X phosphate buffered saline (PBS) for further processing.

Neonatal rat pups were euthanized by decapitation, followed by sternotomy. Pinching the shoulder blades together forced the heart to pass the

chest wall where it was collected, cleaned, and transferred into 1X PBS to remove excess blood prior to decellularization.

To collect fetal rat pup hearts, a pregnant dam was anesthetized with ketamine (100mg/kg) and xylazine (10mg/kg). Hysterectomy was performed, and the fetuses were removed from the placenta. The fetal rat pups were euthanized by decapitation, and their hearts were collected in a similar manner to the neonate pups. This work was performed under a dissecting microscope.

3.2.1.2 Tissue Decellularization and Solubilization

Hearts were decellularized via perfusion or agitation soaking, depending upon the age of the rat. For the adult life point, retrograde perfusion of the aorta (leading to anterograde perfusion of the coronary vasculature) was performed according to previous protocols (16). The tissue was subjected to a 1% sodium dodecyl sulfate (SDS) perfusion until no visible cellular material remained (16-36 hours), then washed with ddH_2O, 1% Triton-X 100, ddH_2O, and 4cycles of 12 hours duration of 1X PBS. Fetal and neonatal hearts underwent the same process but were soaked and not perfused. Since the hearts at these life stages are

considerably thinner, diffusion and convection were adequate for removal of the cellular material from the hearts.

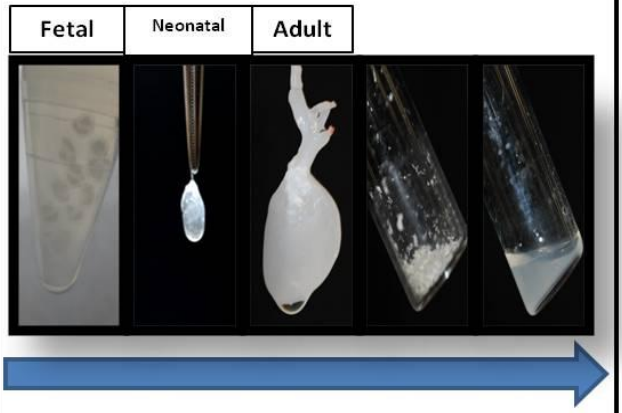

Figure 3-1. Processing of whole organ for solubilization. From left to right: E19 fetal hearts, P2 neonatal heart, adult heart. Cellular material is removed with 1% SDS via agitation (fetal only) or perfusion. The remaining ECM is then solubilized by mechanical disruption, lyophilization, and enzymatic digestion.

Solubilization was achieved by mechanically disrupting the decelled tissue in ddH_2O with a Branson 450 Digital Sonifier (Branson, Danbury, CT). The samples were then lyophilized for 24 hrs and resuspended in 10% pepsin in 0.1M HCl (w/v), and placed on a stir plate for 48 hrs to allow the pepsin to digest the ECM, before being neutralized with 1N NaOH. The solubilized matrix was then either kept at 4°C for immediate use or aliquoted and frozen at -20°C for long-term storage. (Figure 3-1)

3.2.1.3 Mechanical Testing of Tissue

A custom-built mechanical testing setup based on a previously developed

system (135) was used to interrogate the quasi-static elastic moduli of biological tissue and polyacrylamide gel platforms. Portions of the left ventricular free wall tissue were isolated from neonatal and adult life points; whole organ measurements were performed on fetal tissue due to the size of the decellularized heart. The tissue was stretched in the circumferential direction of the heart in a uniaxial manner. The gauge length for all samples was greater than 2mm and thickness and width of the tissue were measured in the unstrained state in order to calculate engineering stress and strain. Similar measurements were performed on polyacrylamide gels of variable stiffness to produce a standard curve of Young's modulus as a function of bisacrylamide percentage. Gels were then produced according to these expected values for the experimental procedures described below.

3.2.2 ECM Protein Characterization by Indirect ELISA

To assay the protein composition of the ECM we used an indirect ELISA method. Briefly, 10μg of solubilized ECM from each life point was adsorbed onto tissue culture plastic overnight in the biosafety hood. The wells were washed three times with 1X PBS to remove non-adsorbed protein. The remaining protein

was then blocked with 5% milk in 1X PBS with tween 20 (PBST) prior to being incubated with a primary antibody for two hours (see Table 3-2 for list of antibodies). The wells were then washed three times with PBST prior to being incubated with a Horseradish peroxidase-conjugated secondary antibody for two hours. Finally the wells were washed three times again with PBST prior to addition of 100 µl of 3, 3', 5, 5'-Tetramethylbenzidine (TMB) (Sigma). The TMB was allowed to react for 30 minutes on the bench top prior to colorimetric assessment on the spectrophotometer at 450 nm absorbance. The reaction was stopped by addition of 100 µl of 1N hydrochloric acid, and the subsequent color change was assessed at 650 nm absorbance. All samples were run in triplicate at a minimum, averaged, and normalized to the fetal life point before being plotted.

3.2.3 Cell Culture Platform

3.2.3.1 Glass Slide Activation

22mm^2 No. 1 glass coverslips were treated to provide stable functional groups for polyacrylamide binding according to established methods (116). The coverslips were first rendered hydrophilic via heat treatment by passing one surface over a flame. The slide was then placed on a piece of parafilm in the

chemical hood, heat-treated side-up. Using two q-tips, a 1N sodium hydroxide solution was applied across the surface and allowed to air dry for 10 minutes. 3-aminopropyltrimethoxysilane was then applied and allowed to air dry for 10 minutes. The slides were then placed into 6 well plates and washed twice for 5 minutes with ddH_2O on an orbital shaker. Following the second wash, the slides were covered with 0.5% gluteraldehyde (~2 ml) and allowed to stand in the chemical hood for 30 minutes. The gluteraldehyde was then removed, and the slides were washed three times with ddH_2O and stored under ddH_2O at 4°C until needed.

3.2.3.2 Cross-linking ECM into Polyacrylamide and Casting Gels

40% polyacrylamide was combined with 2% bis-acrylamide at relative concentrations to produce a range of biologically relevant stiffnesses as determined via mechanical testing measurements described above (Table 3-1). Solubilized ECM and N-hydroxysuccinimide (NHS) were incorporated into the gel at equivalent amounts of 400 μg/ml. NHS is commonly used as a cross linking agent because it is capable of forming a covalent bridge between amine groups, making it ideal for cross-linking protein to polyacrylamide (PAAm) (116). The PAAm-ECM solution was then brought to pH6.8 to increase the cross-linking

efficiency prior to the addition of 10% ammonium persulfate which instigated polymerization of the acrylamide by promoting oxygen radical formation.

Prior to making the gel solution, activated coverslips were removed from their 6 well plates and placed on parafilm within a biosafety cabinet. Once dried by vacuum or evaporation, 40 µl of PAAm-ECM solution were deposited close to the center of the slide. Another 22mm^2 No. 1 glass coverslip that was not activated was then feathered and dropped onto the PAAm-ECM solution. Capillary action and surface tension pulled the coverslips into a matched position, generating 80 µm thick gels, similar to previous studies (15). The gels were allowed to polymerize up to 45 minutes prior to removal of the top, non-activated coverslip, and then were washed and placed into 1X PBS

Polyacrylamide - ECM Recipe	0.05%	0.10%	0.20%
40% acrylamide	250	250	250
2% bis-acrylamide	25	50	100
10x PBS	100	100	100
ECM*	400ug	400ug	400ug
TEMED	2	2	2
1M HCl**	a	b	c
5mg/ml NHS	80	80	80
diH2O**	x	y	z
10% APS	5	5	5
Total ul	1000	1000	1000

Table 3-1. Above is the recipe for making the different stiffness gels. Each percentage corresponds to 8kPa, 25kPa, and 40kPa respectively. *The volume of ECM added is dependent upon its concentration; 400ug should be added for every milliliter made. **These values need to be calculated. 1M HCl should be added until the solution is slightly acidic, ~pH6.8. diH2O should be added to bring the final volume up to 1000ul.

overnight to quench any un-reacted NHS.

3.2.4 MSC Cell Culture

Rat MSCs were obtained from Texas A&M Institute for Regenerative Medicine. PAAm-ECM gels were seeded in 6 well plates at 50,000 cells per gel. They were cultured with recommended MSC maintenance media (20% FBS 1% penicillin/streptomycin in alpha-MEM supplemented with 2% L-glutamine) which was changed every 2-3 days. After the first 24 hours gels were transferred to new plates to minimize soluble factor signaling from MSCs attached to the bottom of the plastic culture well. All experiments were performed with cells between passages 8-10.

3.2.5 Immunohistochemistry

The mesoderm transcription markers Nkx2.5 and GATA4 are commonly used as early indicators of cardiac transcription (106). Downstream markers for cardiac commitment include Mef2C and Tbx5 (109, 111), while the expression of cardiac troponin I (cTnI) and myosin heavy chain (MHC) have been previously used to assess mature cardiomyocytes (111).

To assay the spatial location of the transcription factors within the cell, we carried out immunohistochemistry on a subset of samples. Briefly, samples were fixed with ice-cold methanol for 10 minutes. All samples were blocked with 5% donkey serum for 1 hour, incubated with primary antibody (Table 3-2) in

Primary Antibdoy	Host Animal	Manufacturer	Catalog #
Nkx2.5	Rabbit	Santa Cruz, CA	sc-14033
Gata4	Goat	Santa Cruz, CA	sc-1237
Tbx5	Goat	Santa Cruz, CA	sc-48782
Mef2C	Rabbit	Santa Cruz, CA	sc-13266
Troponin I-C	Rabbit	Santa Cruz, CA	sc-52266
MYH	Mouse	Santa Cruz, CA	sc-20641
Collagen I	mouse	Santa Cruz, CA	sc-166865
Collagen IIIA	mouse	Santa Cruz, CA	sc-271249
Collagen VA	mouse	Santa Cruz, CA	sc-166154
Fibronectin	mouse	Santa Cruz, CA	sc-271098
Laminin	Rabbit	Santa Cruz, CA	sc-20142
Elastin	Goat	Santa Cruz, CA	sc-17580
Periostin	Rabbit	Santa Cruz, CA	sc-67233
Secondary Antibody	**Label**	**Manufacturer**	
anti-mouse	Dylight 549	Jackson Immunoresearch	715-505-151
anti-mouse	Dylight 488	Jackson Immunoresearch	715-485-151
anti-mouse	AlexFluor555	Invitrogen	A31570
anti-mouse	HRP	Jackson Immunoresearch	A626520
anti-goat	Dylight 549	Jackson Immunoresearch	705-505-147
anti-goat	Dylight 488	Jackson Immunoresearch	705-485-147
anti-goat	HRP	Jackson Immunoresearch	A611620
anti-rabbit	AlexaFluor 488	Invitrogen	A21206
anti-rabbit	AlexaFluor 555	Invitrogen	A31572
anti-rabbit	Dylight 488	Jackson Immunoresearch	711-485-152
anti-rabbit	HRP	Jackson Immunoresearch	A656120

Table 3-2. List of primary and secondary antibodies used in this research

0.1% bovine serum albumin for 1 hour at room temperature, washed 3 x 5 minutes with 1X PBS, incubated with appropriate secondary antibodies (Jackson Immunoresearch, West Grove, PA, and Invitrogen, Carlsbad, CA) in 0.1% bovine serum albumin for 1 hour at room temperature, then washed again for 3 x 5

minutes in 1X PBS before being set with Vectashield hardmount containing DAPI (Vector Labs, Philadelphia, PA). All images were taken on an Olympus IX-81 (Olympus Americas, Center Valley, PA).

3.2.6 Image Analysis and Quantification

Immunohistological quantification was performed by a custom built algorithm (pipeline) using the CellProfiler software (Broad Institute, Cambridge, MA). Images were filtered such that background was removed prior to assessing image pixel intensity of computer-derived cell areas. The number of cells per field-of-view varied, but averaged 138 during Week 1, and 33 during Week 3. The pipeline loaded the images from a prescribed folder and first transformed them into grayscale, both as a total image and as individual red, blue, and green channels. The software then applied a threshold to each image, removing the lowest values and rescaling the image from 0-1. This was not always sufficient to remove background for some images, so another filter identified, and removed, the remaining background noise. The program then identified nuclei from the blue (DAPI) channel, and used this as a reference for the “propagate” algorithm, which identified the edges of the cell. Once these cell areas were isolated from

the original image, the intensity of the red and green channels within those individual areas was measured. These individual measurements of cell-localized intensity were then averaged and plotted.

3.2.7 Western Blotting

Western blotting was used to quantify both ECM composition and cell differentiation. Based on the success of the probes utilized for immunohistology, the same primary antibodies were used to interrogate the cell differentiation on nitrocellulose blots. Myosin heavy chain was considered an unlikely success based on size restrictions of the PAAm gels used for PAGE. Ultimately, the blots for cell differentiation were probed for expression of Nkx2.5, Mef2C, and B-actin. For ECM composition we probed the blots for antibodies against collagens I and V, and periostin.

In order to assess the impacts of the PAAm-ECM gel system on stem cell differentiation, cells were lifted at the various time points via trypsanization and then lysed in ice cold lysis buffer (2X NP40, 40X sodium deoxycholate, 100X sodium orthovandate, 1000X aprotinin, 1000X leupeptin, and 1000X pepstatin in

ddH_2O) via sonification. Total protein of the cell lysate, or solubilizied ECM, was quantified using a BCA assay (Thermo Scientific, Pittsburgh, PA). Samples underwent PAGE separation in either 10% PAAm gels, or variable 4-15% gel, with up to 20 μg protein per lane before being transferred to a nitrocellulose membrane. In general, blots were blocked with 5% non-fat milk in tris buffered saline with tween 20 (TBST) for 1 hour, incubated with a primary antibody for 1 hour, washed with TBST (3 x 10 minutes), incubated with an HRP-conjugated secondary antibody for an hour, and then washed again with TBST (3 x 10 minutes) prior to signal detection via chemiluminescence with luminol. Autorad film (Bioexpress, Kaysville, UT) was exposed to the blots for varying amounts of time and the film was developed using a Konica Minolta SRX-101A (Tokyo, Japan), scanned into the computer and quantified with ImageJ (NIH, Bethesda, MD).

3.3 Results

3.3.1 Physical and compositional characterization of Cardiac ECM

In order to assess composition, we performed quantitative indirect ELISA on the ECM components Collagens I, III, and V, Elastin, Laminin, Fibronectin, and Periostin and assessed their relative expression over time (Figure 3-2). The determined values were normalized to their respective average values determined for the fetal life point. Other than Collagen III (and a non-significant dip in neonatal elastin), all other protein

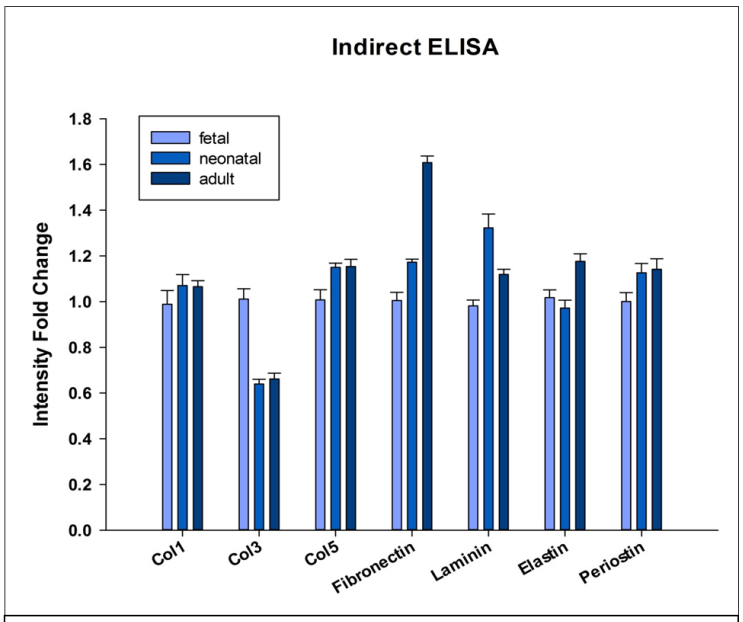

Figure 3-2. Spectrophotometry results of indirect ELISA for relative quantification of decellularized ECM

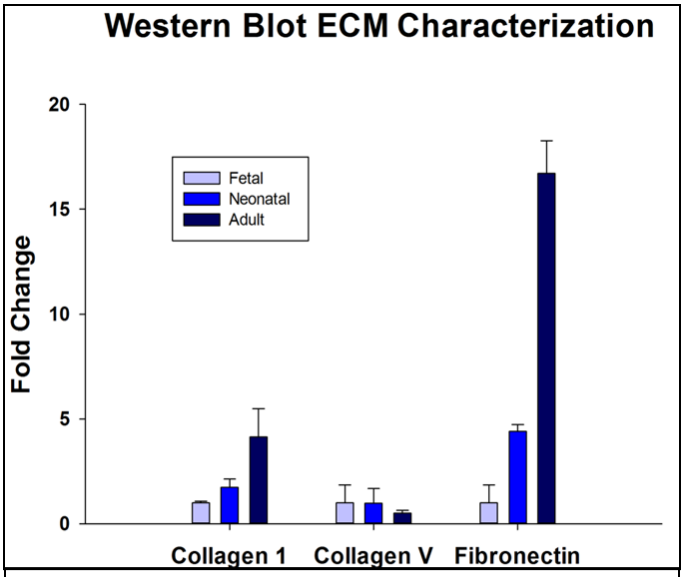

Figure 3-3. Western blot results for semi-quantitative analysis of ECM proteins

concentrations are observed to increase with age.

We also attempted to evaluate the composition of the ECM via Western blotting (Figure 3-3). In experiments performed by Dr. Corin Williams, the relative concentrations of collagen I, collagen V, and fibronectin were assessed by antibody staining. Her results (n=2) indicate a 4-fold increase of collagen I in adult versus fetal ECM, an overall decrease in collagen V, and a 16-fold increase in fibronectin.

3.3.2 MSC Adherence to PAAm-ECM Gels is Comparable to Culture Plastic

Characterizing the native tissue allowed us to produce substrates with similar properties for cell culture. By combining bis-acrylamide at 0.05%, 0.1%,

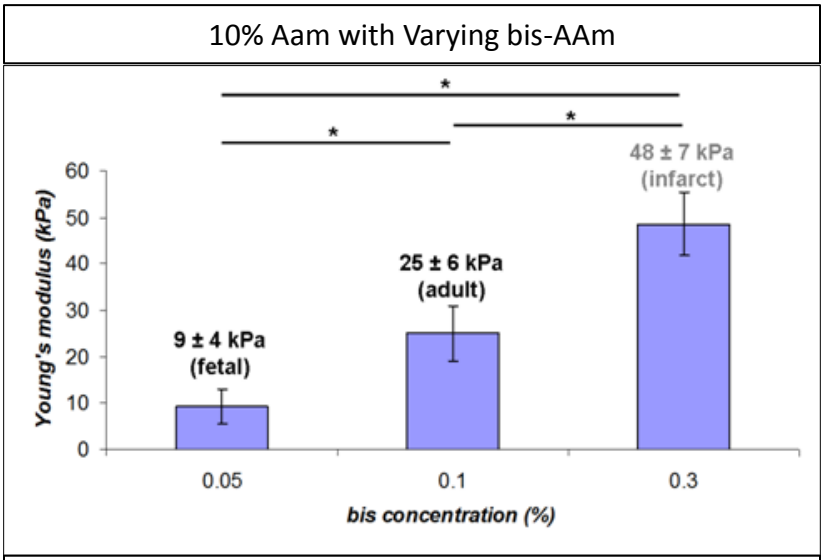

Figure 3-4. Polyacrylamide gels can be generated at physiologically relevant stiffnesses

and 0.2% with acrylamide at X%, we are able to produce PAAm hydrogel of 8+/-1 kPa, 25 +/- 3 kPa, and 40 +/- 6 kPa respectively (Figure 3-4). Cells seeded on the 8 kPa gel resulted in a rounded morphology versus the typical spread morphology seen on stiffer gels and culture plastic. This coincides with previous reports that substrate stiffness is an important factor for attachment that does not appear to be altered by the presence of ECM proteins (15).

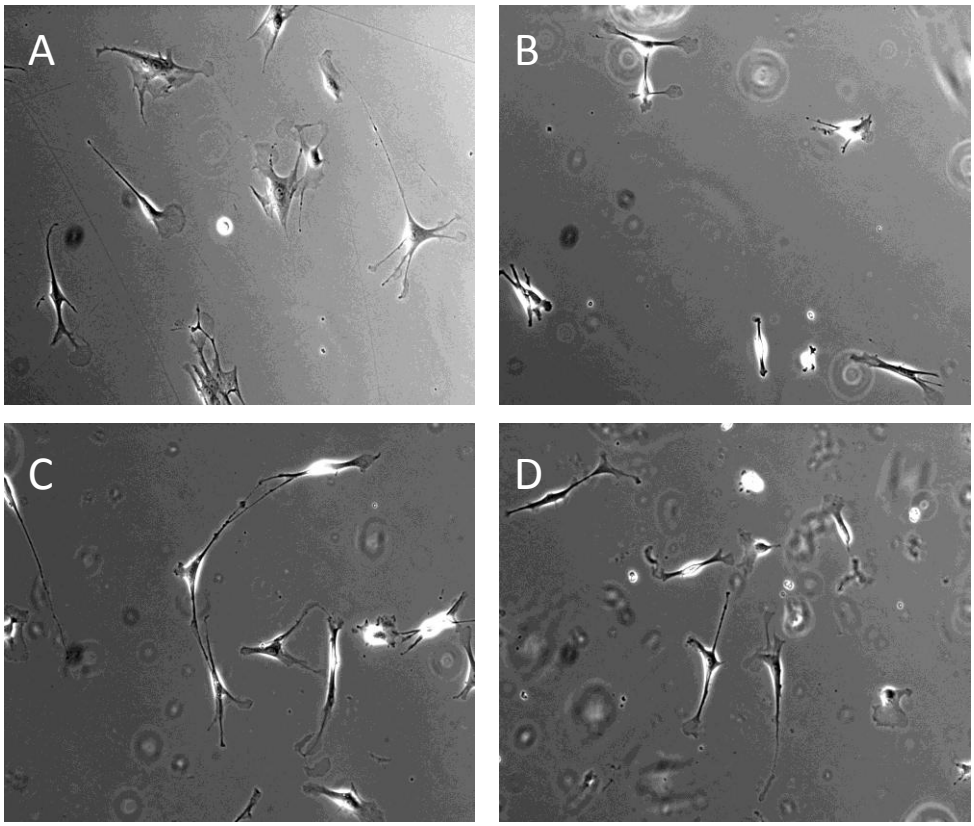

Figure 3-5. Morphological assessment of MSC adherence and spreading on solubilized ECM incorporated in PAAm. *A* depicts MSCs on standard tissue culture plastic. *B-D* show MSC grown on 40kPa PAAm incorporating 20, 80, and 160ul of 5mg/ml solubilized ECM, respectively. No significant difference in shape is seen in *C* v *D*, and both more closely resemble cells on plastic than *B*, confirming 400ug of protein per ml PAAm as an acceptable standard.

Polyacrylamide alone does not provide functional groups for cellular attachment, but by including increasing amounts of solubilized ECM (with a respective increase in NHS), we were able to optimize the surface modification to produce attachment similar to that seen under standard culture conditions (Figure 3-5C).

As can be seen in Figure 3-5, increasing the concentration up to 400 μg/ml provided enough cellular attachment points to allow the seeded cells to attach and spread on 40 kPa gels in a manner similar to that observed on tissue culture plastic (Figure 3-5A).

3.3.3 PAAm-ECM Histology show Rapid Induction of Cardiac Markers

The ability of the gels to influence cardiogenesis was qualitatively assessed by immunohistochemistry probing for the cardiac markers described above. Figures 3-6 to 3-11 show representative images of matched transcript staining (columns) on all possible combinations of stiffness (rows) for each life stage of ECM composition. Where background staining is evident, it is attributed to incomplete wash-out of secondary antibodies prior to entrapment within the PAAm-ECM under the Vectashield hardmount.

At 1 week (Figures 3-6 to 3-8), cells appear attached and well spread. There is strong signal detected, although at various levels across conditions. Nkx2.5 is easily visible at 8 kPa and 25 kPa for fetal and neonatal, but only observed at 40 kPa in adult composition. GATA4 has peri-nuclear coexpression

with Nkx2.5, but only in fetal and neonatal compositions at 25 kPa. Tbx5 and Mef2C demonstrate fluctuations in expression, but nevertheless can be detected across all conditions. Mef2C appears to localize in a punctate manner within the cell pseudopodia. cTnI is observed in most conditions, but the brightest signal appears at neonatal 25 kPa, followed by adult 25 kPa. The only condition that lacks cTnI, but shows MHC staining, is neonatal 40 kPa.

By 3 weeks (Figures 3-9 to 3-11), a significantly different staining profile is evident. There are considerably less cells per field-of-view, and, in general, these exhibit a diminished level of staining when compared to the above. The cells do not demonstrate the same level of attachment and spreading, rather it appears that the remaining cells have grown off the gel into 3D bodies, anchored by a small support structure. The most notable signaling is detected in the neonatal 8 kPa condition, for Nkx2.5, Mef2C, and cTnI. However, staining for Nkx2.5 and cTnI is relegated to the edge of the 3D mass.

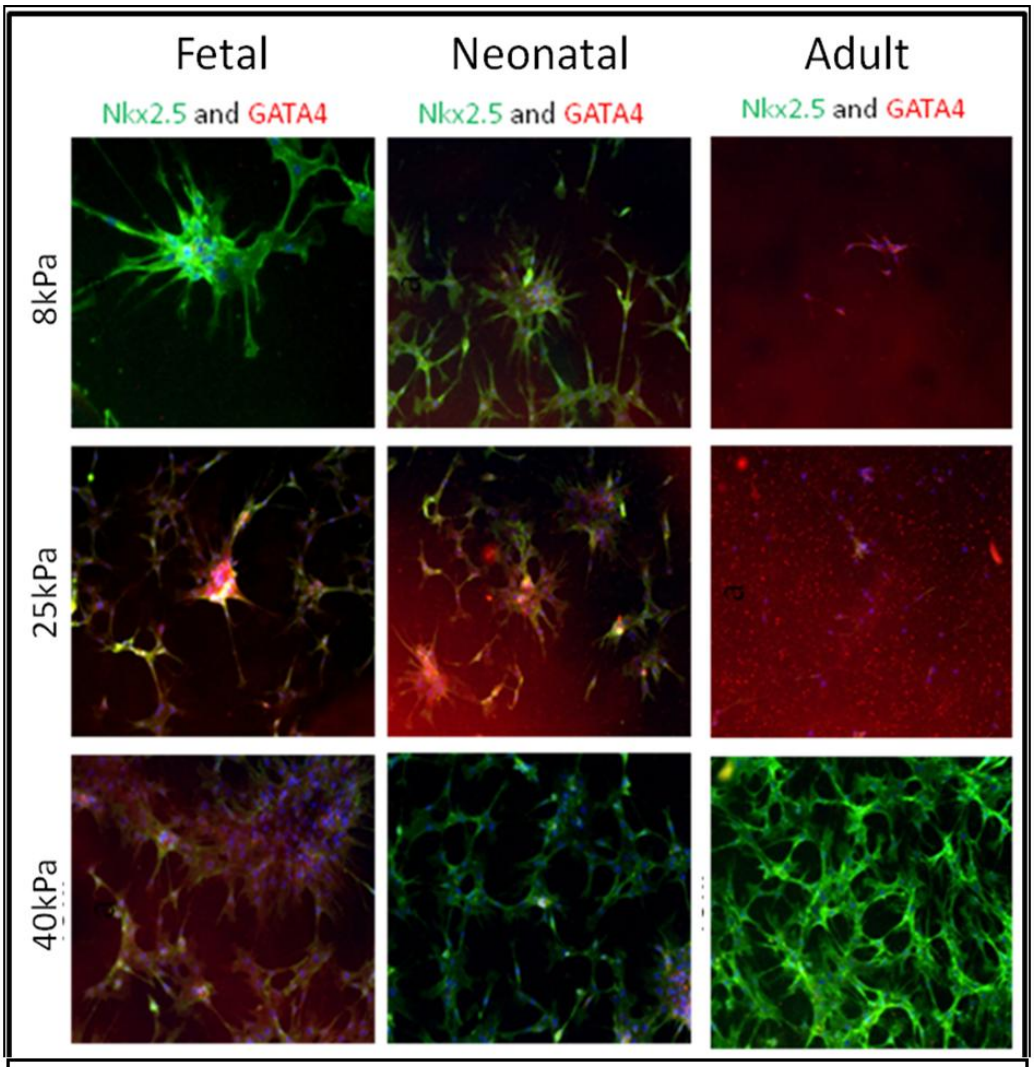

Figure 3-6. Depicts immunohistology for Nkx2.5 (green) and GATA4 (red) across all three stiffnesses and compositions at 1 week. The top row depicts cells grown on 8kPa gels; the middle row on 25kPa gels; the bottom row on 40kPa gels. The left column shows cells grown on fetal ECM; the middle column on neonatal ECM; and the right column on adult ECM. All nuclei are labeled with DAPI (blue).

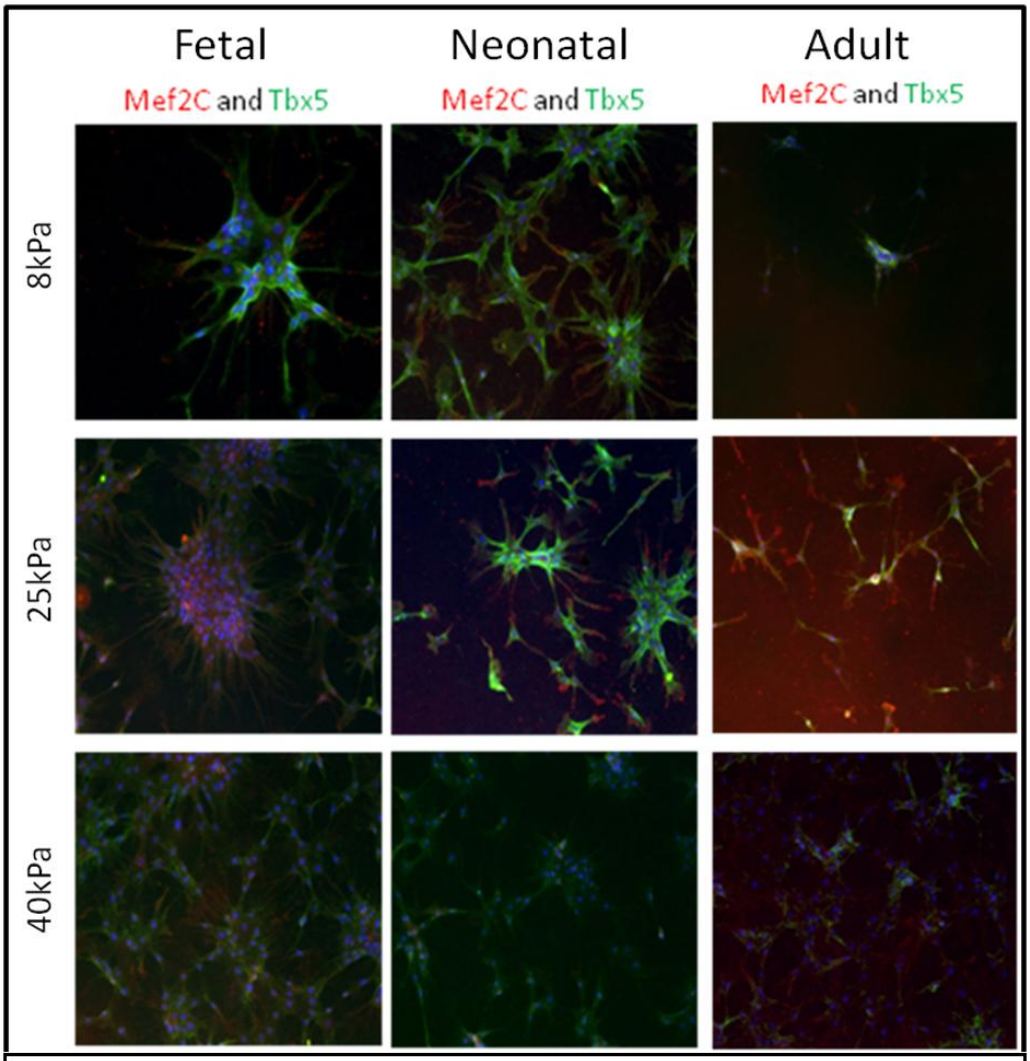

Figure 3-7. Depicts immunohistology for Tbx5 (green) and Mef2C (red) across all three stiffnesses and compositions at 1 week. The top row depicts cells grown on 8kPa gels; the middle row on 25kPa gels; the bottom row on 40kPa gels. The left column shows cells grown on fetal ECM; the middle column on neonatal ECM; and the right column on adult ECM. All nuclei are labeled with DAPI (blue).

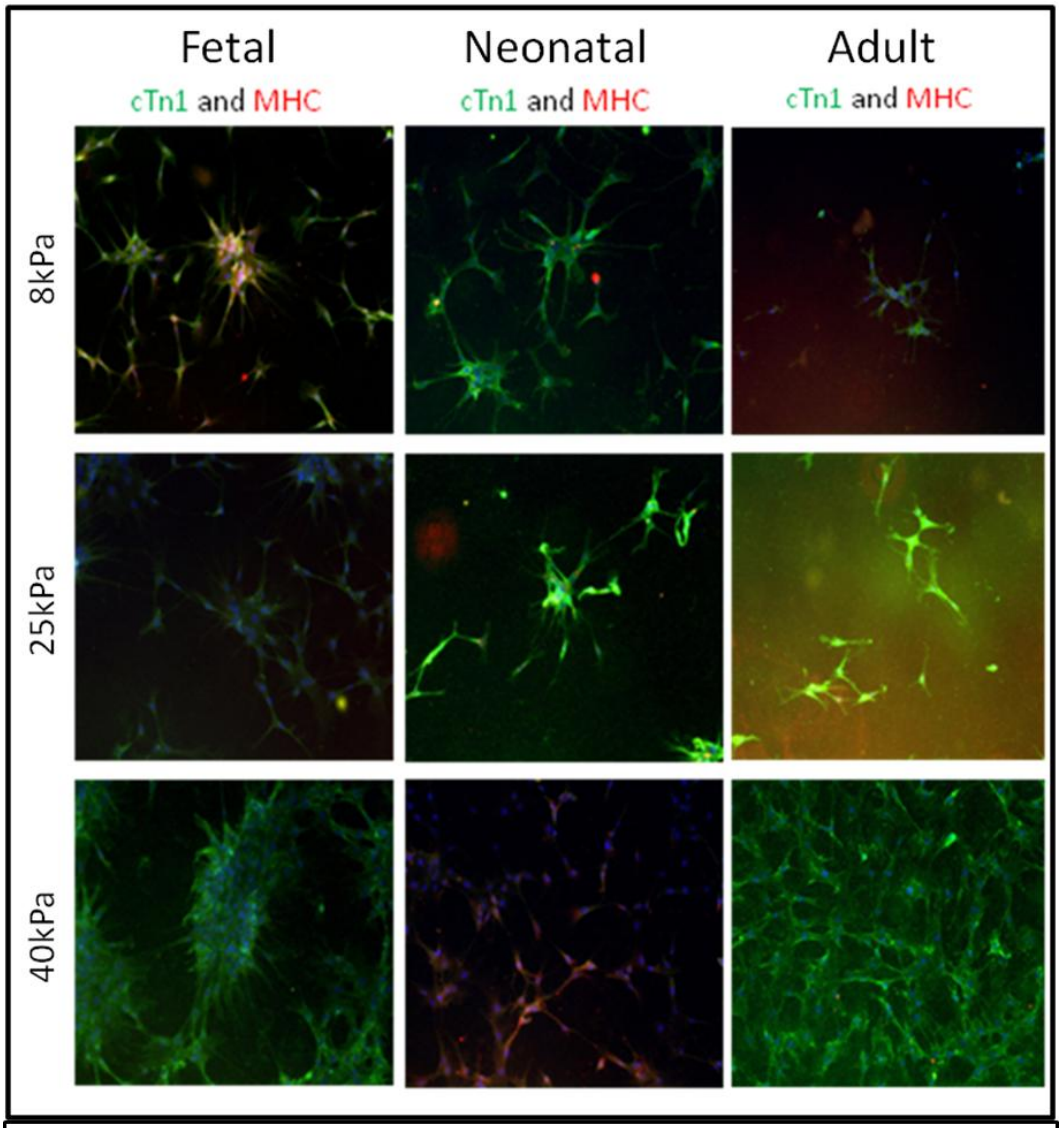

Figure 3-8. Depicts immunohistology for cTnI (green) and MHC (red) across all three stiffnesses and compositions at 1 week. The top row depicts cells grown on 8kPa gels; the middle row on 25kPa gels; the bottom row on 40kPa gels. The left column shows cells grown on fetal ECM; the middle column on neonatal ECM; and the right column on adult ECM. All nuclei are labeled with DAPI (blue).

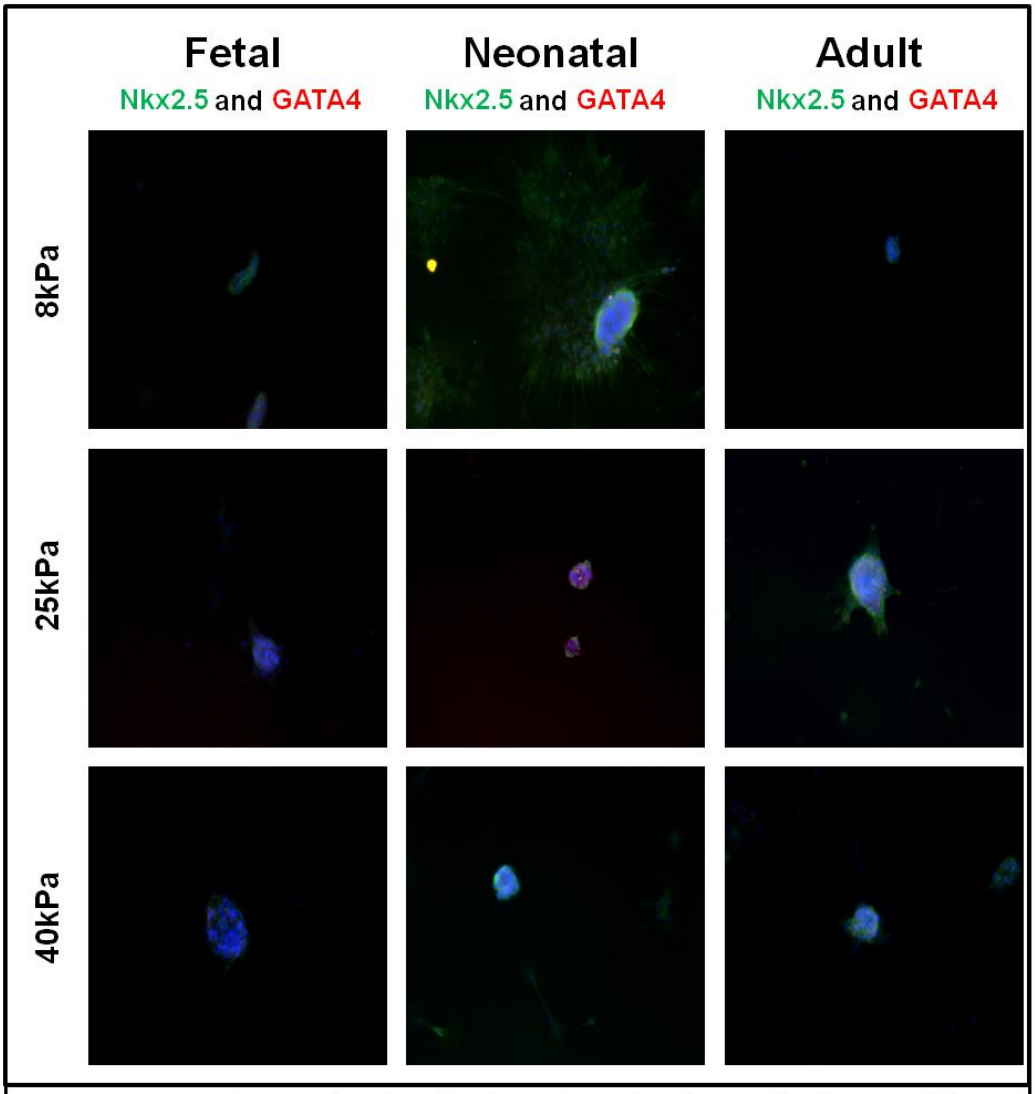

Figure 3-9. Depicts immunohistology for Nkx2.5 (green) and GATA4 (red) across all three stiffnesses and compositions at 3 weeks. The top row depicts cells grown on 8kPa gels; the middle row on 25kPa gels; the bottom row on 40kPa gels. The left column shows cells grown on fetal ECM; the middle column on neonatal ECM; and the right column on adult ECM. All nuclei are labeled with DAPI (blue).

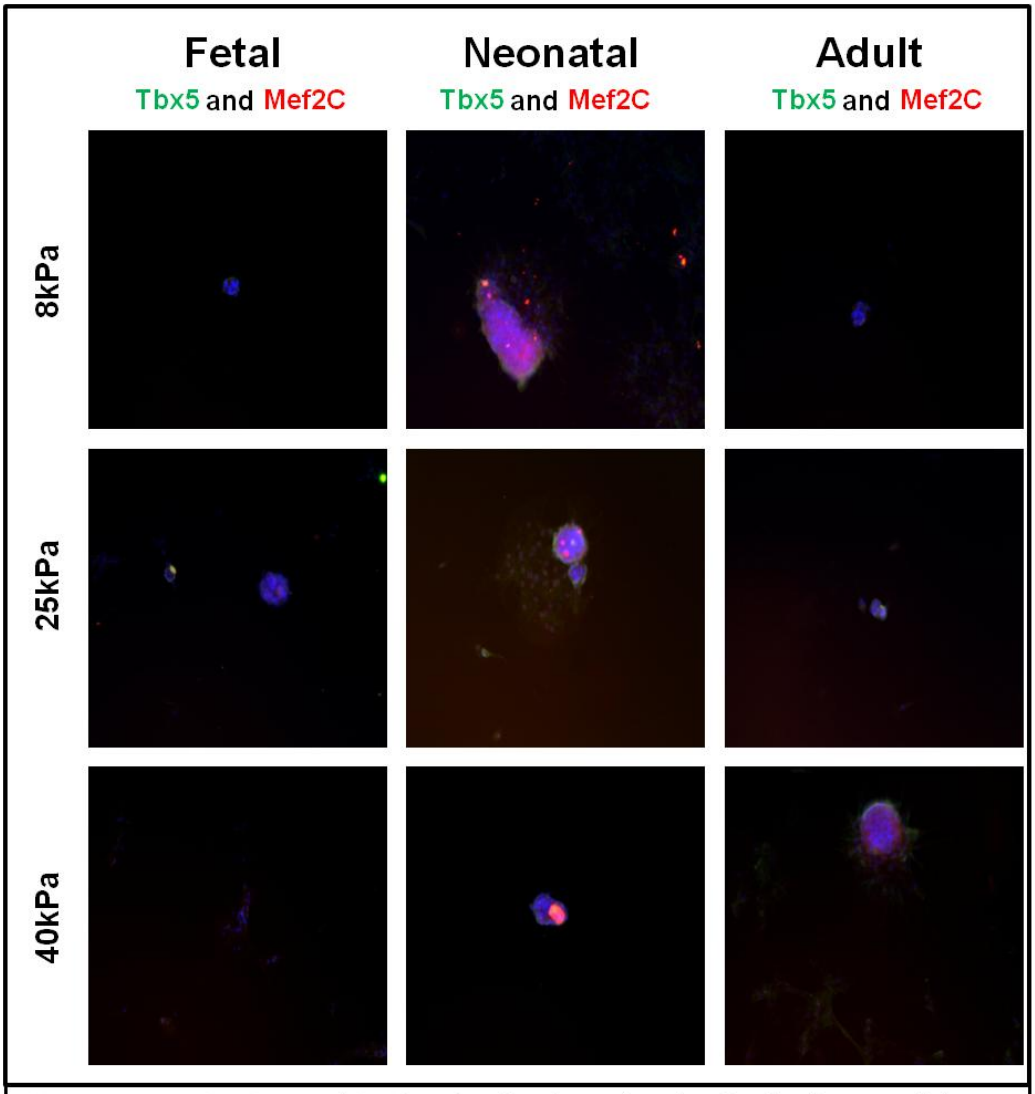

Figure 3-10. Depicts immunohistology for Tbx5 (green) and Mef2C (red) across all three stiffnesses and compositions at 3 weeks. The top row depicts cells grown on 8kPa gels; the middle row on 25kPa gels; the bottom row on 40kPa gels. The left column shows cells grown on fetal ECM; the middle column on neonatal ECM; and the right column on adult ECM. All nuclei are labeled with DAPI (blue).

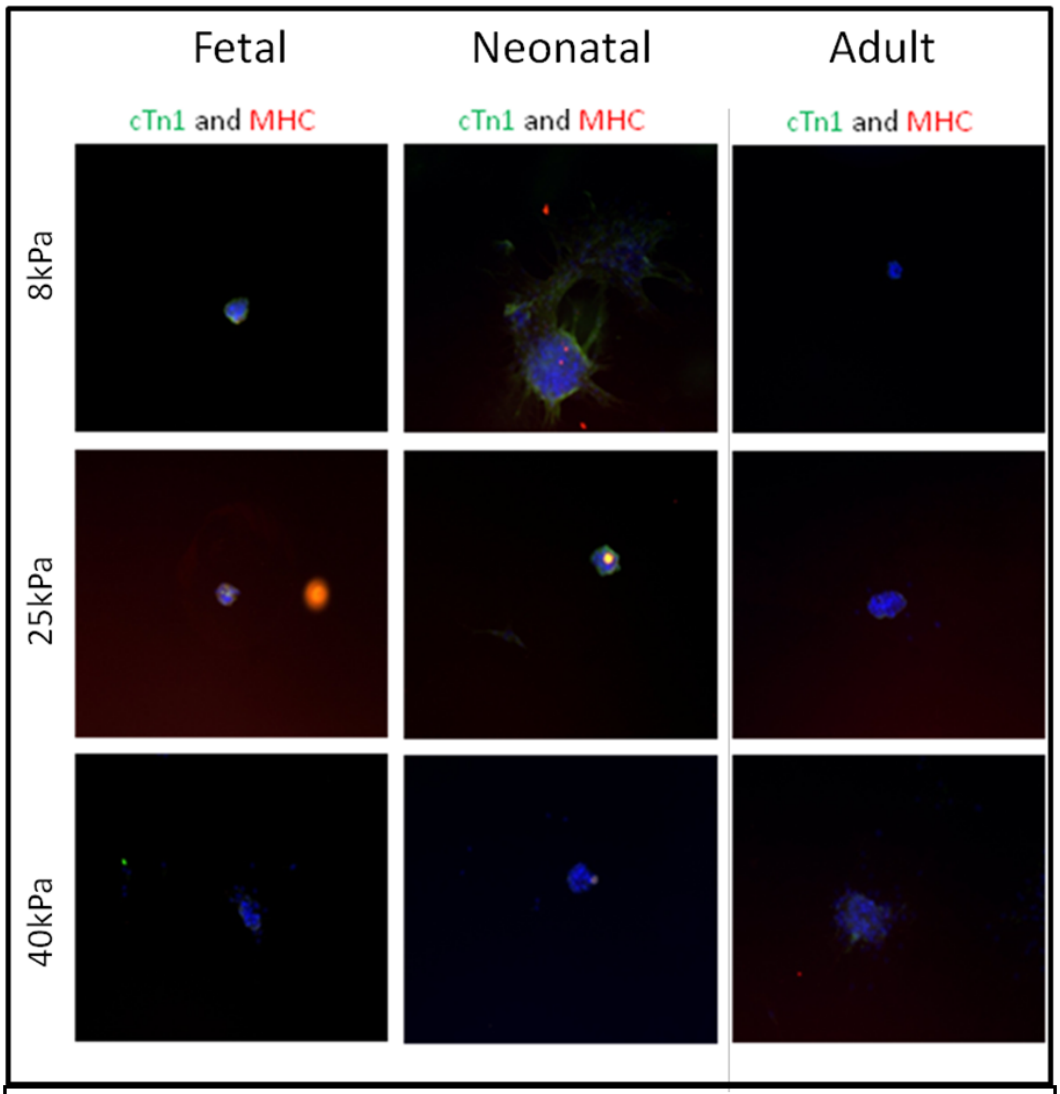

Figure 3-11. Depicts immunohistology for cTnI (green) and MHC (red) across all three stiffnesses and compositions at 3 weeks. The top row depicts cells grown on 8kPa gels; the middle row on 25kPa gels; the bottom row on 40kPa gels. The left column shows cells grown on fetal ECM; the middle column on neonatal ECM; and the right column on adult ECM. All nuclei are labeled with DAPI (blue).

3.3.4 Image Analysis Confirms Complex Effects of Stiffness and Composition

To quantitatively evaluate the fluorescent signal detected, we used CellProfiler to filter out background and measure signal from each color channel expressed within the automatically determined cell area. Concurrent with the above observations regarding immunohistology, quantitative fluorescent signal at 1 week is 2 to 10 fold higher than at 3 weeks. At 1 week, the highest cardiac marker expression was observed in the physiologically relevant stiffnesses of 8 kPa (associated with neonatal) and 25 kPa (associated with adult). The very early transcription marker Nkx2.5 has a significantly greater expression ($p<0.05$) at 8 kPa over 25 kPa and 40 kPa when coupled with fetal and neonatal composition. However, when cultured on adult ECM, Nkx2.5 has minimal expression at 8 kPa and 25 kPa, but very large expression at 40 kPa (Figure 3-14). Moving down the transcription pathway, the strongest expression (per composition group) is almost always found at the 25 kPa stiffness (Figure 3-12). Interestingly, when the composition groups are compared against each other (within markers), “Adult” expression is significantly higher ($p<0.05$) in the cardiac development transcript Tbx5, and the cardiac maturation markers cTnI and MHC (Figures 3-15 and 3-16).

At 3 weeks, all cells have demonstrated a dramatic decrease in cardiac marker expression except for the mature markers cTnI and MHC (Figure 3-13). Similar to week 1, in general the greatest expression of cTnI and MHC (per composition group) is found at the physiologically relevant stiffnesses 8 kPa and 25 kPa. In contrast to week 1, these Fetal and Neonatal groups demonstrate significantly higher expression ($p<0.05$) than the Adult, a reversal of the expression (Figure 3-19). It is interesting to note that fetal-8 kPa maintained a relatively high level of MHC expression throughout the timecourse.

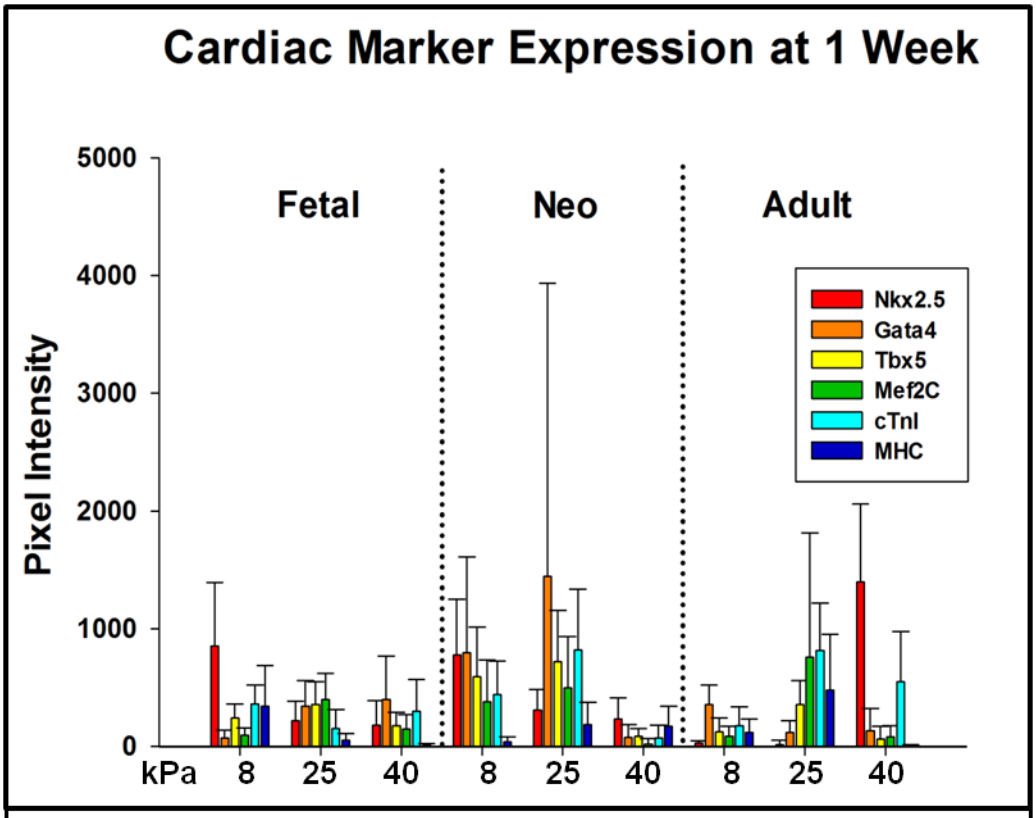

Figure 3-12. Compiled data showing all expression markers grouped by substrate-composition combinations. Average n = 139.

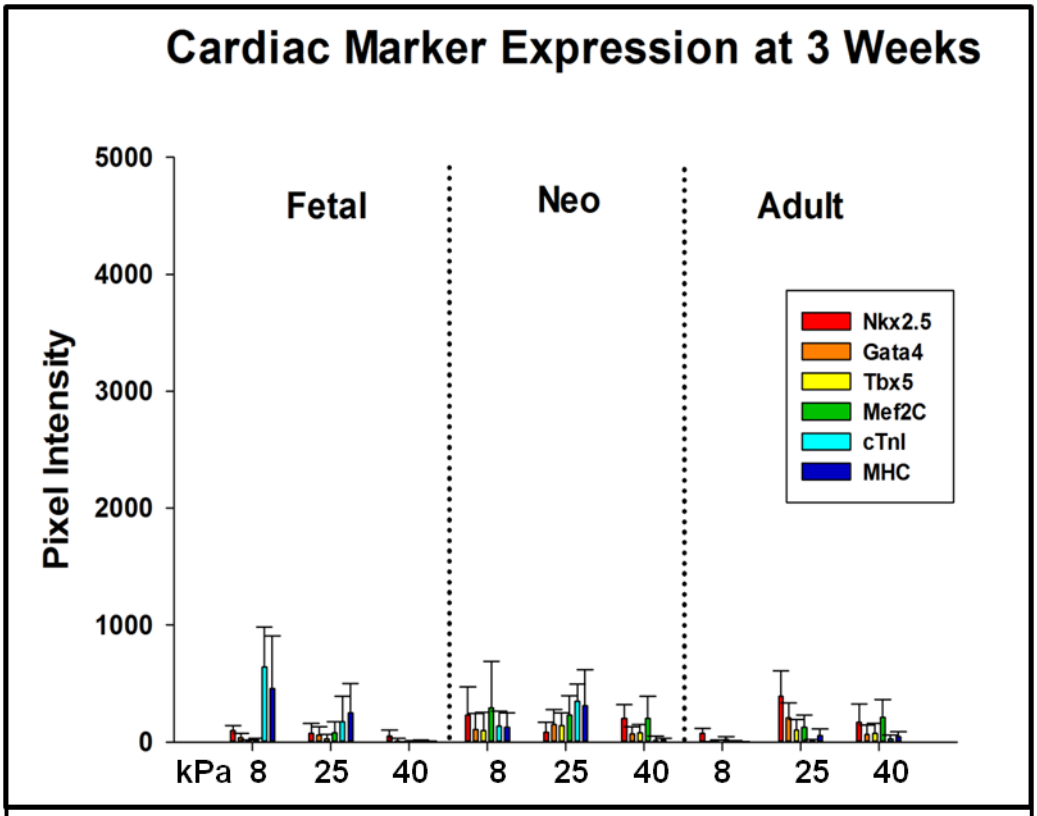

Figure 3-13. Compiled data showing all expression markers at 3 weeks grouped by substrate-composition combinations. Average n = 139.

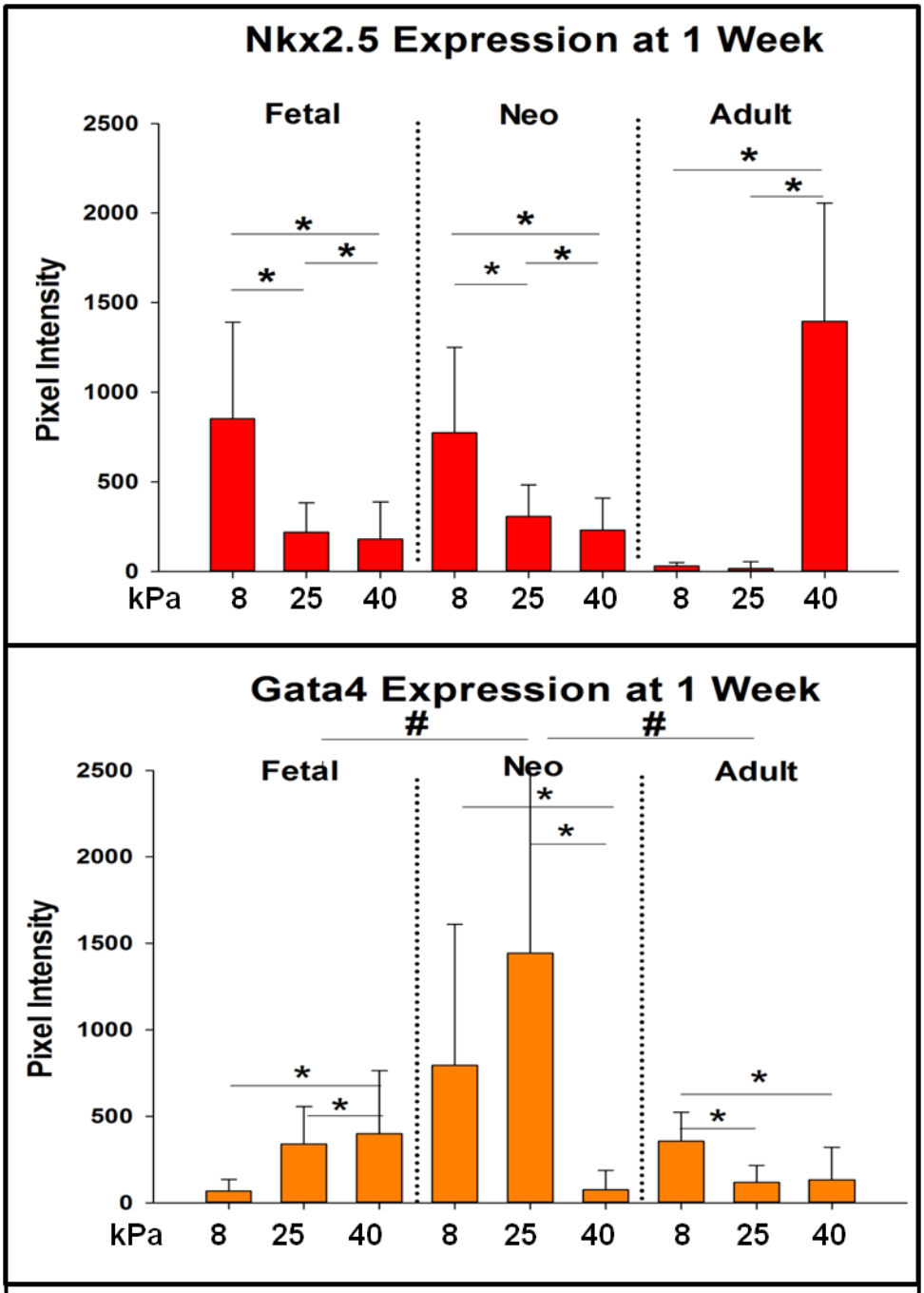

Figure 3-14. Quantitative histology showing cardiac marker expression at 1 week for Nkx2.5 (A) and Gata4 (B). Average n = 139. Significance ($p<0.05$) between stiffness indicated by *, between compositions indicated by #.

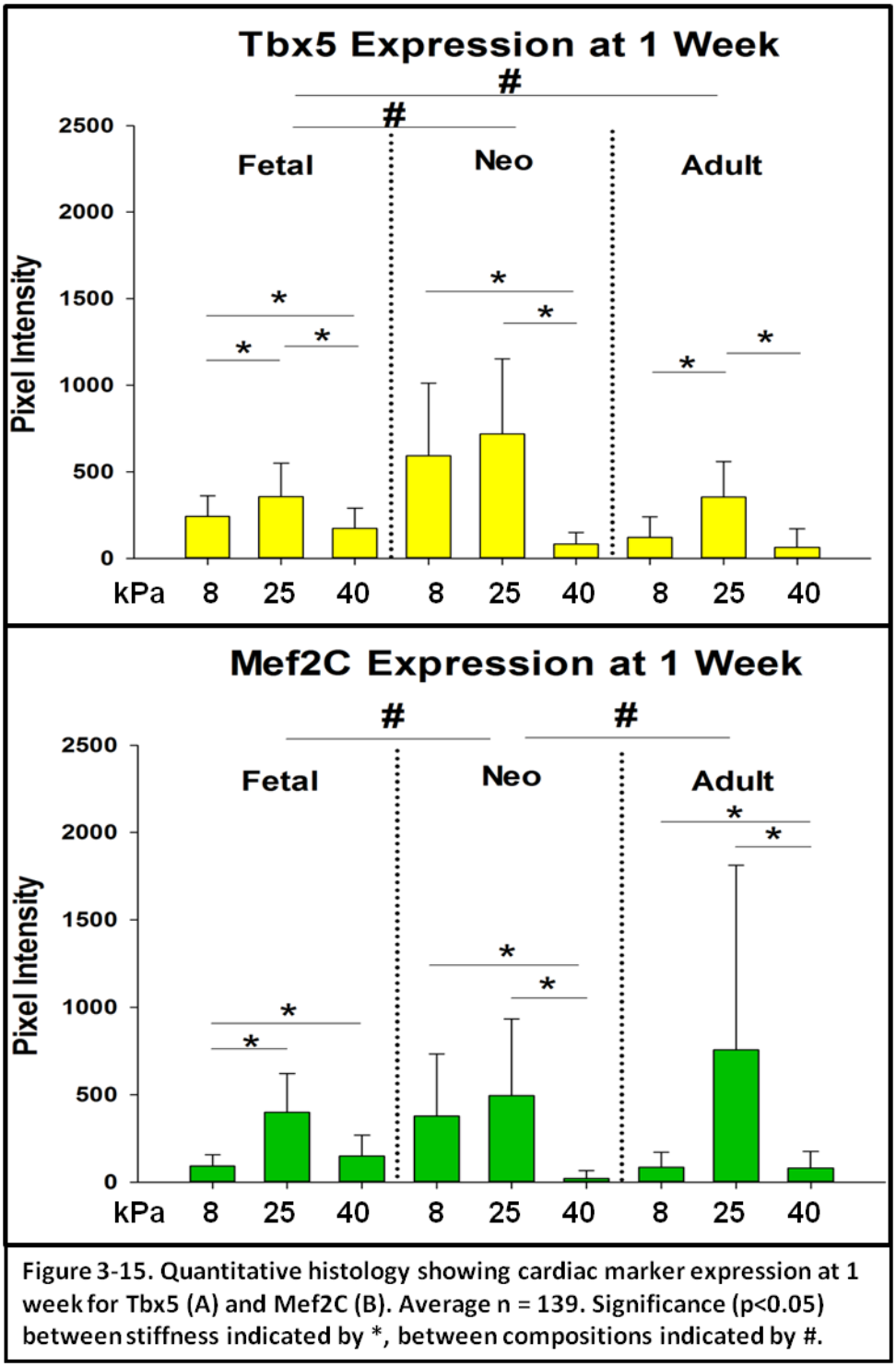

Figure 3-15. Quantitative histology showing cardiac marker expression at 1 week for Tbx5 (A) and Mef2C (B). Average n = 139. Significance ($p<0.05$) between stiffness indicated by *, between compositions indicated by #.

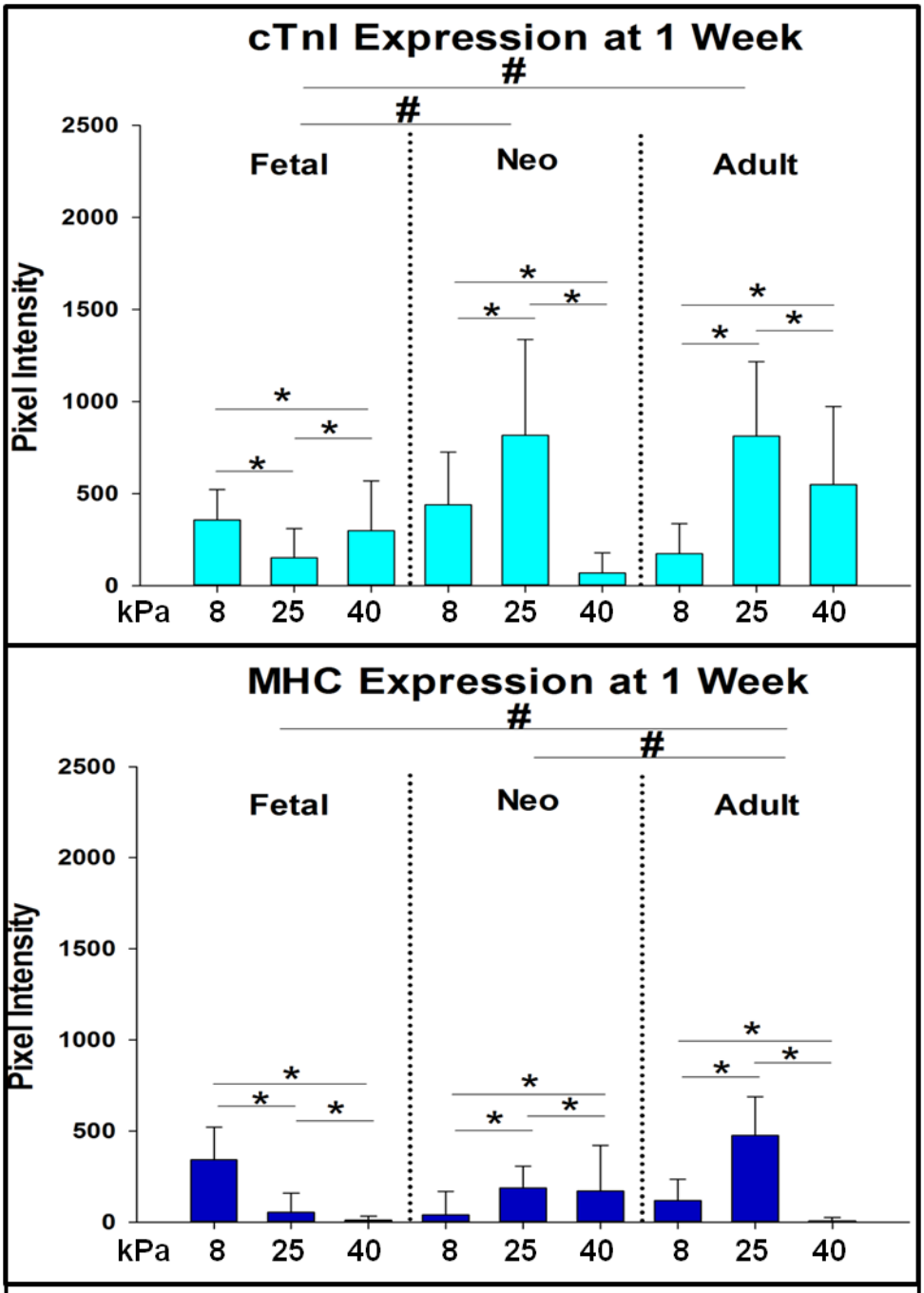

Figure 3-16. Quantitative histology showing cardiac marker expression at 1 week for cTnI (A) and MHC (B). Average n = 139. Significance ($p<0.05$) between stiffness indicated by *, between compositions indicated by #.

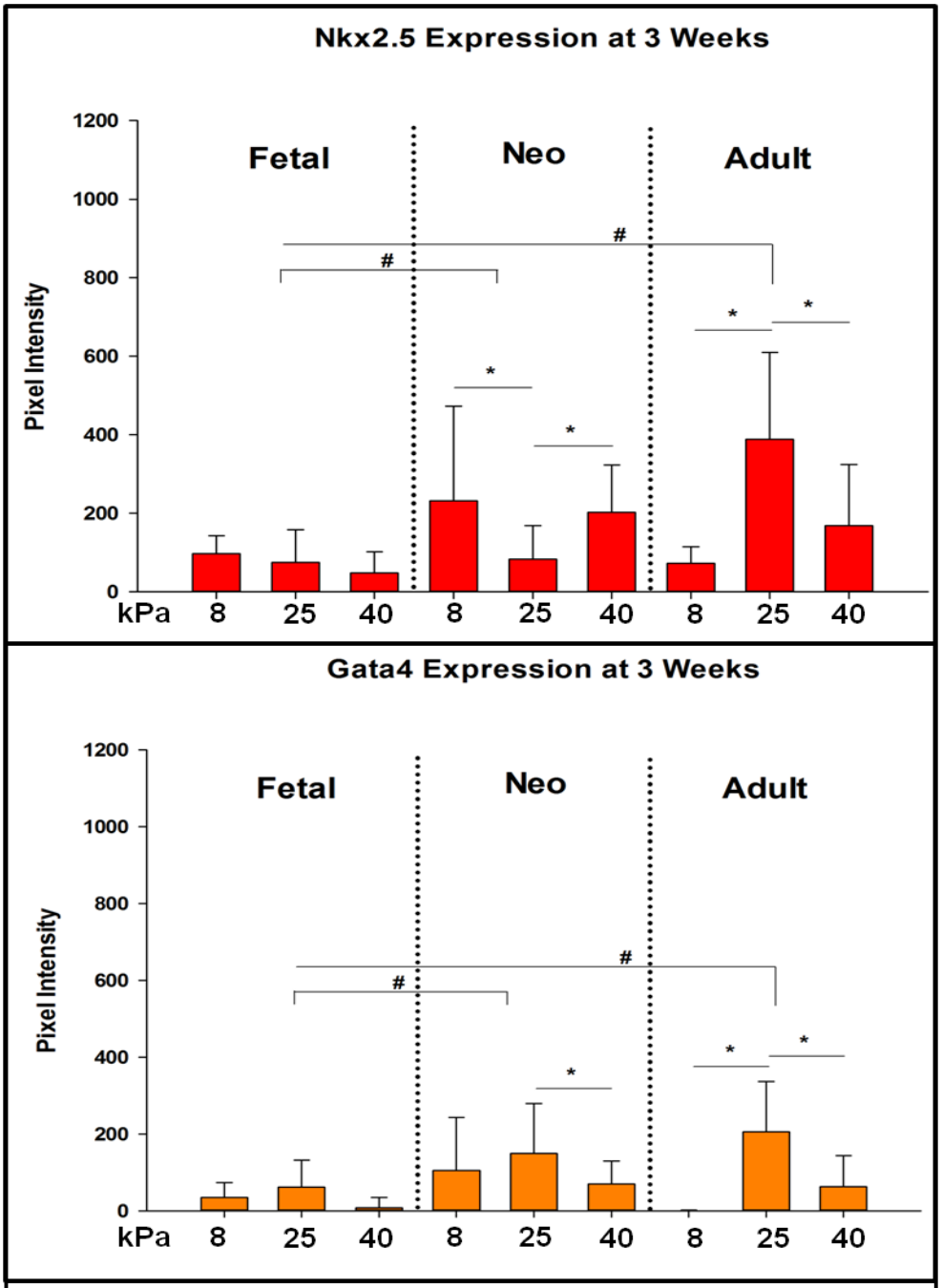

Figure3-17. Quantitative histology showing cardiac marker expression at 3 weekS for Nkx2.5 (A) and Gata4 (B). Average n = 139. Significance ($p<0.05$) between stiffness indicated by *, between compositions indicated by #.

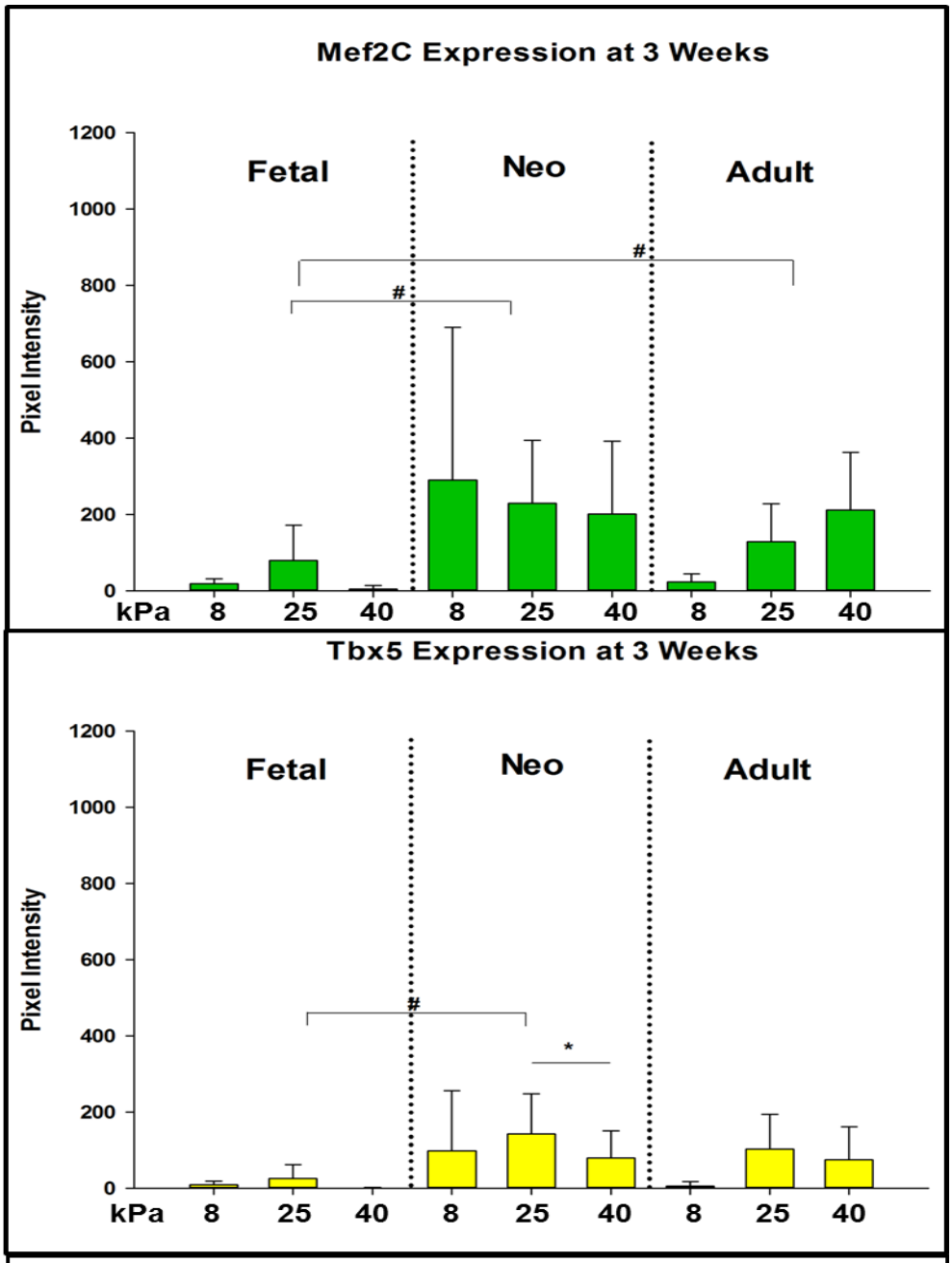

Figure3-18. Quantitative histology showing cardiac marker expression at 3 weekS for Mef2C and Tbx5. Average n = 30. Significance ($p<0.05$) between stiffness indicated by *, between compositions indicated by #.

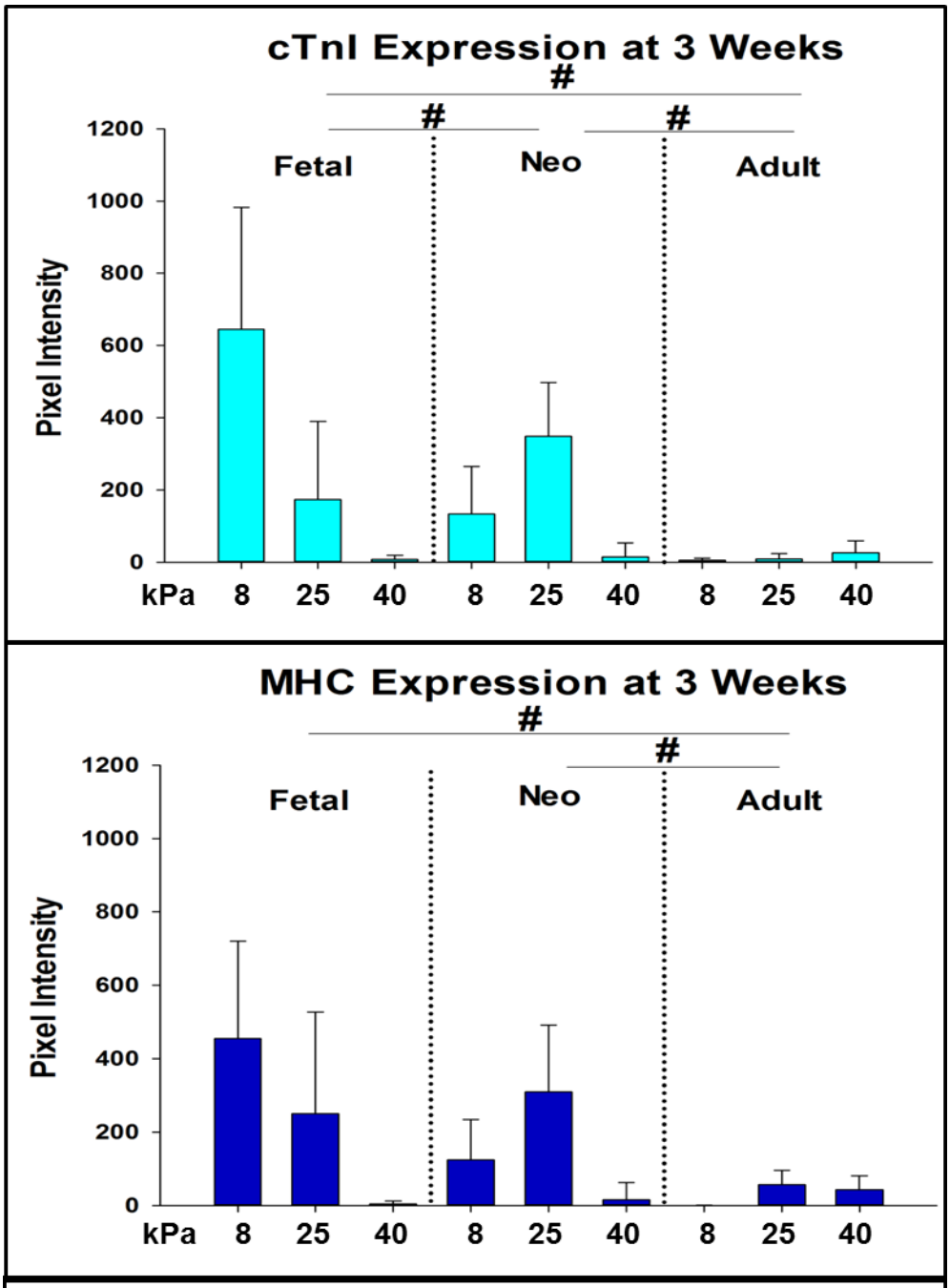

Figure3-19. Quantitative histology showing cardiac marker expression at 3 weekS for cTnI and MHC. Average n = 30. Significance ($p<0.05$) between stiffness indicated by *, between compositions indicated by #.

3.3.5 Western Blot Stiffness vs. ECM Composition

Western blotting was also used to quantify the cardiac transcription factors induced by the various substrate combinations. The final films were quantified using ImageJ, and detected proteins were normalized to their respective β-actin expression. Due to the limits of the comb-size, samples were grouped by experimental timepoint in duplicates, allowing for inter-life point direct comparison (Figure 3-20).

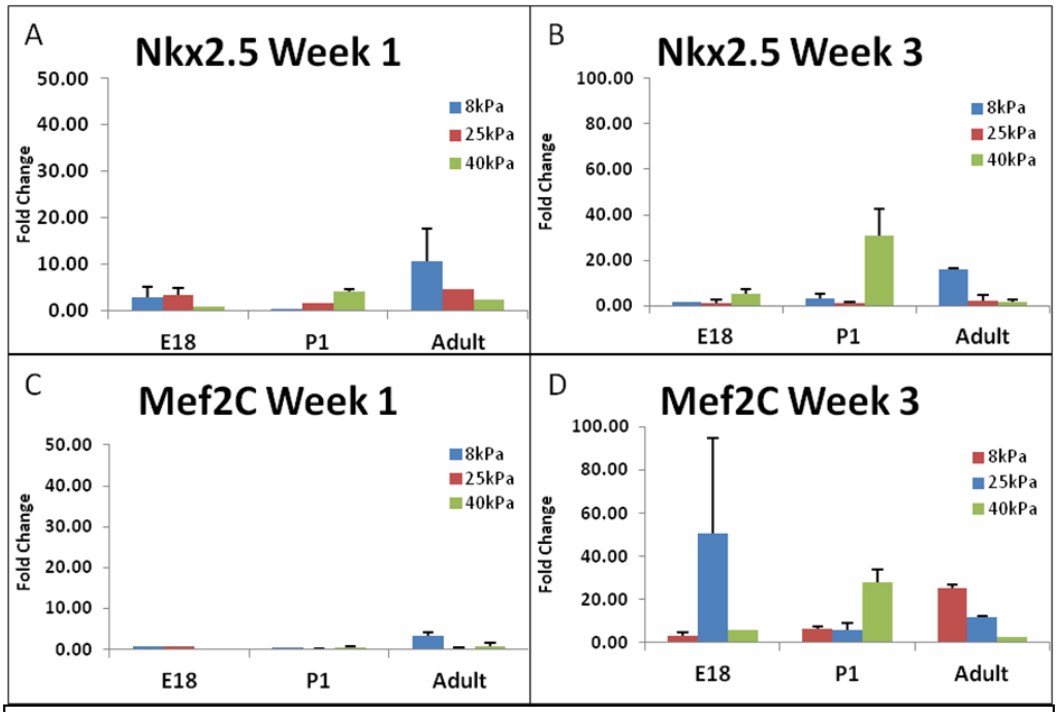

Figure 3-20: 1 week Western blot data for (*A*) Nkx2.5 and (C) Mef2C at, and 3 week Western blot data for (B) Nkx2.5 and (D) Mef2C. All data is normalized to β-actin, n=2.

The results demonstrate that samples cultured on adult ECM at 8 kPa demonstrate the highest level of Nkx2.5 when compared to any other life point (Figure 3-20). Moreover, Nkx2.5 expression on adult composition appears negatively modulated as a function of increased stiffness, but this trend is reversed for neonatal ECM. Interestingly, Nkx2.5 expression on fetal 8 kPa and 25 kPa gels does not appear to be different when compared to neonatal 40 kPa and adult 25 kPa gels. At 3 weeks, neonatal 40 kPa Nkx2.5 has increased by roughly 6 fold. Fetal 40 kPa gels have also demonstrated increased Nkx2.5 expression of approximately 2 fold. However, the alternate conditions demonstrate no significant variability over time. This implies that developmentally immature ECM can be positively modulated by increased stiffness. However, more data is required to verify these preliminary findings.

Mef2C showed relatively little expression at 1 week across the sample set, except for adult 8 kPa. By 3 weeks, Mef2C expression had increased across the board, the most dramatic belonging to fetal 25 kPa, neonatal 40 kPa, and adult 8 kPa.

3.3.6 Alternate ECM Source Do Not Upregulate Full Component of Cardiac

Genes

To evaluate whether MSC cultured on ECM derived from an alternate source would undergo cardiac induction, we cultured cells on PAAm-ECM gels with bovine skeletal muscle incorporated as the ECM. The samples were assessed at 1 week via the same CellProfiler pipeline above. The results (Figure 3-21) demonstrate that skeletal muscle was capable of inducing Nkx2.5 and GATA4; however, the validity of this data should be questioned, as their error bars are larger than the mean indicating that the result is likely noise in the measurement. Likewise, the strong Tbx5 signal on 40 kPa stiffness is the result of too much background (as determined by further investigation into the image analysis), and if those data are removed, demonstrates minimal fluorescence concurrent with the other transcription factors. Perhaps most importantly, for Nkx2.5 and cTnI, zero fluorescent signal was detected at 8 kPa and 40 kPa. It appears that skeletal

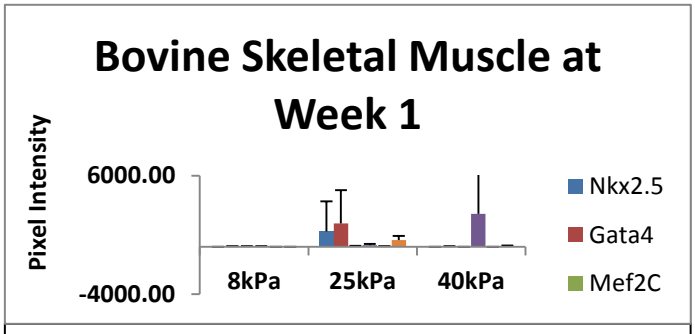

Figure 3-21: Pixel intensities calculated by CellProfiler. The transcription factors are in order from left to right Nkx2.5, Gata4, Mef2C, Tbx5, cTnI, and MHC. They are grouped from left to right at 8kPa, 25kPa, and 40kPa.

muscle is only capable of inducing very early cardiac transcription markers (if at all), but not markers of mature cardiomyocytes, and even then only at physiologically relevant stiffness.

Additional experiments examined the ability of single ECM proteins to induce cardiac differentiation as a function of stiffness. Gels of 8, 25, and 40 kPa were constructed that contained collagen I, collagen V, or fibronectin respectively. Figure 3-22 shows representative images wherein no evidence of the cardiac markers is observed on MSC cultured at 25 kPa, and similar results were observed across all culture conditions (data not shown).

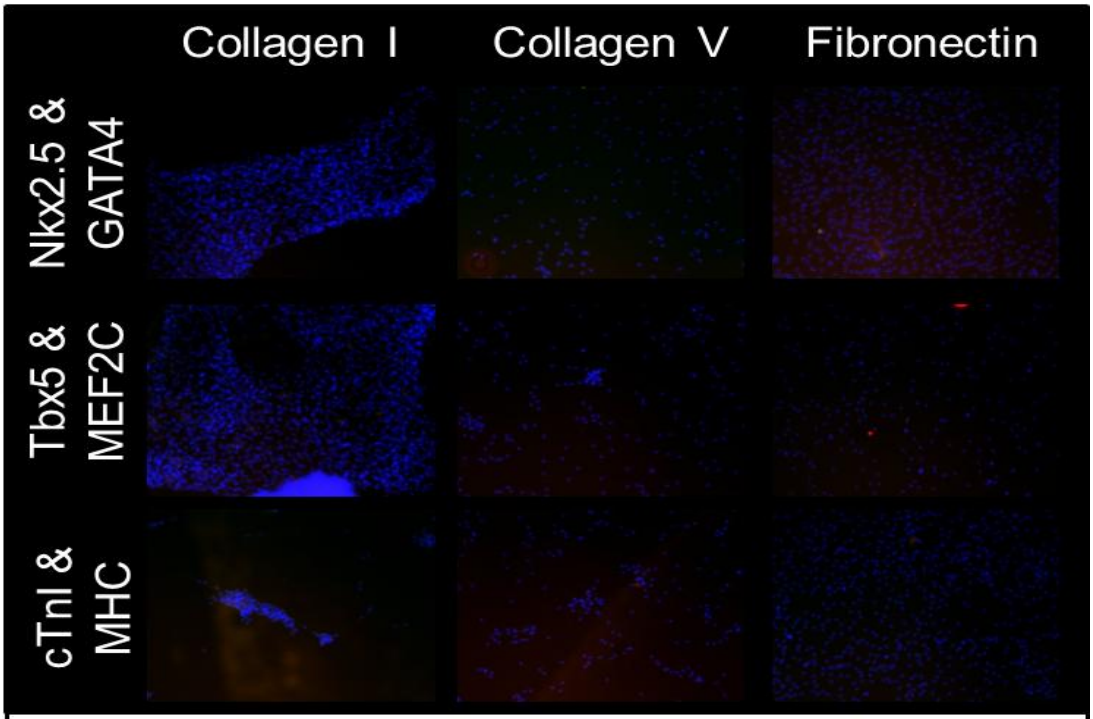

Figure 3-22. Representative image showing lack of cardiac markers in cells cultured on singular the singular ECM proteins Collagen I (left), Collagen V (middle), and Fibronectin (right) on 25 kPa at 1 week. Cells cultured on 8 kPa and 40 kPa gels demonstrated similar results (data not shown).

3.4 Discussion

The goal of this study was to assess the ability of stiffness coupled decellularized ECM to induce MSC cardiac differentiation. To investigate this we first characterized the uniaxial mechanical force of rat hearts from specific life stages, and then generated PAAm gels of physiologically relevant stiffnesses with incorporated solubilized cardiac ECM from each those same life stages. This matrix of stiffness versus composition allowed us to decouple these critical ECM properties and explore their respective importance in transcriptional activation. To evaluate the MSC response to the culture substrate, we utilized quantitative immunohistology and Western blotting to probe for known markers of cardiogenic differentiation and maturation. Our results indicate that stiffness and composition interact in a complex manner to induce MSC differentiation, and that this approach has potential as a method to promote MSC cardiogenesis *in vitro* in the absence of soluble factors. The specific findings of this work are discussed in more detail below.

In our assessment of ECM ELISA, we observed a trend of highly variable results that make it difficult to rely on this approach to deduce the true composition of ECM at different life points. As can be seen in Figures 3-23 and 3-

24, there is a high variability between ELISA assays utilizing different ECM sources. Although some variability is expected, in some cases the opposite result is displayed. Part of this discrepancy is most likely attributable to variability in the adsorption of ECM proteins to the culture plastic well (Figure 3-23). As indicated by the yellow arrows, this variability exists within the replicate, which limits the usefulness of this data. Furthermore, our alternate investigation into ECM proteins conducted via Western blot demonstrated disagreeing results of collagen I concentration increases of 4-fold (Figure 3-3), and an overall decrease in collagen V. However, the trend in fibronectin expression appears similar. The disparate nature of these results decreases our confidence in the usefulness of indirect ELISA as a method to perform semi-quantitative analysis of ECM proteins, further exacerbated by the fact that the observed changes in collagen I, collagen III, collagen V, and periostin with age conflicts with previous work (55). This disparity could arise

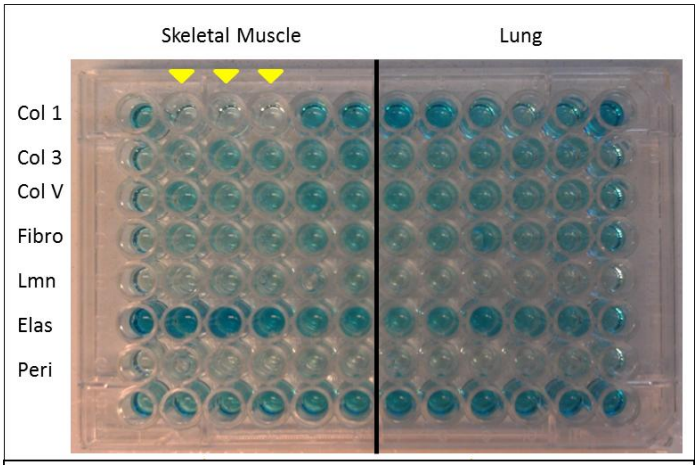

Figure 3-23. Indirect ELISA showing variability of protein adsorption within replicates. Each Ab interrogated row contains 6 replicates for either bovine skeletal muscle, or rat lung. Yellow arrows indicate examples of high-variability within a replicate set.

from the need to use the whole fetal and neonatal heart, but only the adult ventricles are interrogated. Furthermore, it could be a limitation of the volume of ECM required for either approach; the small size of the neonatal and fetal hearts requires them to be pooled as a group, while the large adult ventricles can be solubilized alone. Future experiments should combine multiple adult hearts to limit any possible outlier observations.

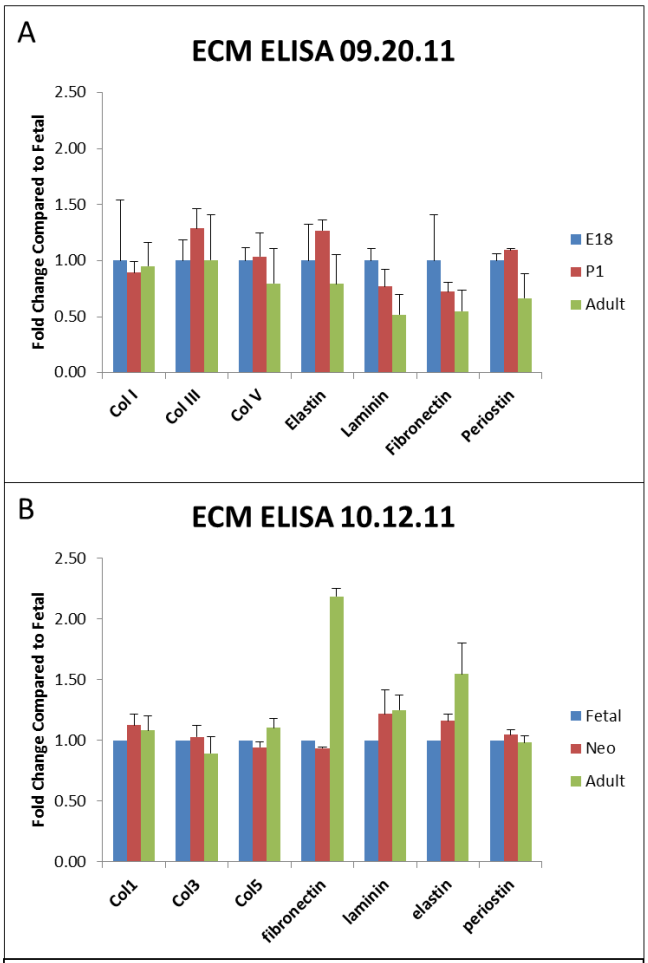

Figure 3-24. Representative examples demonstrating the high variability between indirect ELISAs run from the same sample source.

Genotypic and phenotypic response of pluripotent stem cell differentiation as a function of substrate stiffness has been previously reported (11, 15, 73, 75, 141). Knowing that the cardiac mechanical environment changes over time (136), we designed our PAAm gels on stiffnesses associated with

different stages of cardiac development, similar to other investigations that have demonstrate myogenic and cardiomyogenic differentiation (11, 15, 141). The data derived from our quantitative immunohistochemistry shows that MSC cardiogenesis is evident across all substrate combinations, but, as expected, is generally inhibited by the infarct-associated stiffness. However, this disagrees with the cardiac marker expression profile determined by Western blotting. This could be due to the small amount of data points for each group in the Western blot analysis. Blots had to be constructed that contained 2 lanes per sample due to a limited amount of starting material and a large amount of samples investigated. This limits the statistical applicability of this data, and in the future this should be addressed by an increased amount of repeats. Additionally, these data were collected from two independent experiments, which could impact their comparison.

In our immunohistological assessment of cardiac differentiation, the genetic transcription markers Nkx2.5, Gata4, Tbx5, and Mef2C were all expressed at various levels throughout the cell. Nkx2.5 was detected in a punctate manner within the nuclei, but demonstrated a notable expression within the cytoplasm. Although this has been previously reported (137), functional Nkx2.5 is normally translocated to the nuclei (137). At present it

remains unclear why such a strong cytoplasmic localization of Nkx2.5 was observed. Our results demonstrating localization of Mef2C and Tbx5 in the cytoplasm support previous research implicating FAK-mediated Mef2C activation (117) and Tbx5 association with cytoskeleton actin filaments (140). cTnI and MHC had an observed expression, but lacked the organization normally associated with mature contractile apparatus (111, 112). As expanded upon below, this might be due to the fact that the cell that has not fully entered a mature phenotype.

Our quantitative results appear to indicate that the strength of the cardiac marker expression can be correlated to the composition of the substrate and modulated by stiffness. Nkx2.5 demonstrates a polarized expression, showing strongest on fetal and neonatal groups at 8 kPa, but strongest in the adult group at 40 kPa. The similar expression profiles seen for the fetal and neonatal groups might be a function of our samples' life points; the E19 fetal pups and P1 neonatal pups are roughly 2-3 days apart in age. The spike in Nkx2.5 expression on the adult composition at 40 kPa might be attributable to MSCs instigating cardiac wound healing, as has been implicated in the conserved Nkx2.5 homeobox analog Tinman in *Drosphilia* (134). The downstream markers trend toward greater expression on 25 kPa gels, specifically that of Mef2C and

cTnI. Mef2C is required for proper cardiac development and is only expressed at basal levels within a mature heart (110); cTnI is a cardiac-specific troponin required to form the functional unit that prevents actin-myosin cross-linking in the absence of calcium (2), but the cultured MSCs were never observed to contract. Taken together, the relatively high expression of these two markers could indicate a cell population that was mostly, but not completely, differentiated toward a functional cardiomyocyte as has been reported by others (62, 66)

At 3 weeks (Figure 12-14) there was an observed decrease in overall cell number (data not shown) and marker expression. The decrease in cell number is likely explained by the lack of polyacrylamide functional groups, which inhibits the ability of MSCs to remodel their local environment by depositing new matrix proteins (116) and results in their detachment from the PAAm surface over time. The observed decrease in signal is not a function of the decreased cell number as the signal was calculated on a per cell basis. Given that total gestation of a rat is 21 days, and that cTnI and MHC demonstrate consistent expression across the experiment, it seems most likely that the remaining cells have moved down the transcriptional pathway toward a more terminally differentiated state. However, it is evident from the histology (Figures 3-9 to 3-11) that, at 3 weeks, the cells are

no longer spread and have formed 3D aggregates. This morphology, taken with the above knowledge of the changes in the surface protein, make it difficult to assert what level of ECM mediated signaling is occurring at this timepoint. This discontinuous signaling could potentially be part of the reason why that, even at 3 weeks, no cells were observed to spontaneously contract.

If stiffness or composition was solely responsible for directing MSC differentiation, our observed results should correlate directly to previous studies demonstrating directed differentiation (11, 15, 17, 22, 23, 75), but they do not. The high degree of cardiac marker expression variability suggests that stiffness and composition do act together to regulate cardiac induction of MSCs. The lowest stiffness (8 kPa, associated with developing heart) was better for supporting the early transcription factor Nkx2.5, but 8 kPa and 25 kPa (associated with a mature healthy heart) demonstrated better expression for downstream transcription markers; in most cases, 40 kPa (approximately the stiffness of an infarct) negatively modulated expression. This appears to implicate composition as the more important factor for differentiation. It does appear to be synergistically modulated by the corresponding life point associated stiffness. For example, MSCs, per composition group, express the most significant ($p<0.05$) amount of Tbx5 when neonatal ECM is coupled with

25kPa (Figure 3-15). A similar observation can be seen in the mature MHC marker; the greatest MHC expression is observed when adult ECM is coupled with 25kPa. Furthermore, while the results of incubating MSCs on bovine skeletal muscle do demonstrate some early transcription factor induction, the large error bars indicate that this is most likely a false artifact. None of the downstream markers representing cardiac lineage commitment are detected at levels similar to those observed on cardiac ECM, implicating the importance of the composition to aiding in directing differentiation, supporting the results determined by previous studies (22-24). This data is derived from a limited number of proof-of-concept experiments, and further investigation is required to verify our findings.

This cell culture platform demonstrates a novel *in vitro* method for inducing cardiogenesis in MSCs, without the addition of soluble factors, as a function of their local environment. It advances the concept of ECM-mediated cell signaling, and offers a new method for interrogating the differentiation ability of stem cells. Future experiments should probe the synergistic (or antagonistic) effects of soluble factors, and explore methods to increase the functional culture time to greater than 1 week. This could potentially be achieved by developing a bis-acrylamide analog that contained a non-binding

peptide chain, theoretically providing an attachment point for newly deposited ECM proteins. Other experiments based on this platform could examine other relevant combinations of stiffness and ECM to explore potential synergy across tissue types. It would be very interesting to evaluate the ability of these cardiopoeitic MSCs to function as a cell source for artificial heart tissue. If future investigations can demonstrate complete maturation at high levels of efficiency, this approach holds promise as a therapeutically viable, patient-specific method to generate cells for cell-based therapies.

4. Mesenchymal Stem Cell Proliferation and Differentiation on Integrin-binding Peptide Modified Surfaces

4.1 Introduction

Integrins are transmembrane obligate heterodimer proteins composed of an alpha and beta subunits that are non-covalently associated. They are the main membrane-protein by which cells adhere to the proteins of the extracellular matrix (ECM). There are 18 alpha subunit isoforms and 8 beta subunit isoforms, however, only 24 paired heterodimers have been identified (102). Currently there are three major families based on their beta subunit: cytoadhesion receptors (beta3) (104), leukocyte adhesion receptors (beta2) (103), and very-late-antigen receptors (beta1) (103).

Despite efforts characterizing integrin-protein associations (51-58, 102-104), there is little published data on identified peptide-binding domain sequences for specific integrins. It remains unclear as to why integrins are capable of binding multiple (synergy) domains, but investigation into how these binding events might modify or alter ECM-derived signaling is underway (70). Despite evidence linking focal adhesion kinase to intracellular signaling (91), how specific integrin heterodimers transduce mechanical information is not well

understood.

In an effort to explore this area we chose 4 previously identified integrin binding domains from the literature and assessed their effect on MSC proliferation and/or differentiation. We accomplished this by collaborating with the lab of Professor Qiaobing Xu, based on their expertise in chemically modifying surfaces. The peptides chosen were RGD, TTSWSQCSKS (TTS), SINNNRWHSIYITRFGNMGS (SIN), and FQGVLQNVRFVF (FQG). They are known to bind the integrins α5β1 (118), α6β1 (119), α7β1 (120), and α3β1 (121), respectively, and have been demonstrated to be important in early cardiac development and later cardiac remodeling (142). It is important to note that these experiments were conducted with the help of my undergraduate assistant David Sutherland. He produced Figures 4-1 and 4-2.

4.2 Methods

4.2.1 Peptide Modified Gold Surface

A standard method for immobilizing chemicals (organic and otherwise) of interest to a substrate relies on the modification of a gold surface by utilizing the

naturally occurring semi-strong gold-sulfur bond (17). This technique has been employed in a variety of forms to produce self-assembled monolayers for biological applications (17). For our purposes, we used a NanoMaster NSC-3000 (NanoMaster, Inc) to sputter-coat glass microscope slides with a 20nm +/- 5 thick gold depositions. The slides were then cut with a handheld glass cutter into 33 squares, measuring approximately 7mm per side. The squares were investigated under microscope, and those that had surface deformities (such as scratches or nicks) were discarded. Usable squares were then transferred into a 24 well plate wherein they were covered with isopropanol overnight to sterilize. Afterwards the isopropanol was removed and the plate was sealed with parafilm until it was to be used.

The peptide sequences of 4 previously identified integrin-binding domains (IBD) were altered by the addition of a cysteine amino acid on the carboxyl-oriented end. They were ordered from GenScript (Piscataway, NJ), and guaranteed at >98% purity. Upon receipt they were solubilized in 200 proof ethanol (Sigma) per the manufacturer's instructions, and stored at -20°C between uses. Triethylene glycol mono-11 mercaptoundecyl ether (TGMME) was used as a non-binding negative control (138). Chemical modification of the squares was accomplished by applying approximately 50 µl of 1mg/ml IBD to the

gold (upper) surface and reacting overnight in a biosafety hood. Non-bound peptide was washed away by rinsing the squares three times with PBS prior to seeding the squares with MSCs.

4.2.2 MSC Culture

Rat mesenchymal stem cells were obtained from Texas A&M Institute for Regenerative Medicine. Gold slides were seeded in 24 well plates at 10,000 cells per well. Although the significant height of the gold-covered glass slides had potential to interfere with the initial attachment, this was not observed. The MSCs were cultured with recommended MSC maintenance media: 20% FBS 1% penicillin/streptomycin in alpha-MEM supplemented with 2% L-glutamine, changed every 2-3 days. After the first 24 hours slides were transferred to new plates to minimize soluble factor signaling from MSC attached to the bottom of the plastic culture well. All experiments were performed with cells between passage 8-10.

4.2.3 Morpholigical Assessment

While RGD has been extensively used in a variety of applications to tether cells to surfaces (17, 78, 118), questions remained surrounding the adhesion properties of the other IBDs, the effect of the thiol modification, and the resulting surface presentation of the IBDs based on the thiol location. The ability of the MSC to attach and proliferate was assessed by a standard morphological assay using a light microscope.

4.2.4 Attachment and Proliferation

To assess attachment and proliferation, cell nuclei were stained with Vectashield hardmount containing DAPI (Vector Labs) and imaged on an Olympus IX 81 fluorescent microscope (Olympus Americas). Five fields-of-view were randomly selected by Metamorph (Molecular Devices, Sunnyvale, CA) software for image acquisition and analysis. Data was taken on days 4 and 7. The images were counted manually wherein a nuclei undergoing division was considered a single cell. Likewise, individual images per sample group were manually viewed to assess attachment and spread and all observations were recorded.

4.2.5 Immunohistochemistry

To assess possible mechanotransduction induced transcription, we probed the MSCs at 4 and 7 days with primary antibodies against Nkx2.5 and GATA4. These markers have previously been used to indicate cardiac induction (106). Samples were fixed with ice-cold methanol for 10 minutes at 4°C. The methanol was removed, and the samples were washed 3 x 5 min with 1X PBS prior to blocking with 5% donkey serum for 1 hour. They were stained with primary antibody in 0.1% bovine serum albumin for 1 hour at room temperature, washed 3 x 5 minutes with 1X PBS, and incubated with appropriate secondary antibodies (Table 3-2) in 0.1% bovine serum albumin for 1 hour at room temperature. Another 3 x 5 minute wash with 1X PBS was performed before being set with Vectashield hardmount containing DAPI (Vector Labs). All images were taken on an Olympus IX-81.

4.2.6 Histology

To evaluate the potential of the IBDs to influence MSC differentiation

toward adipocytes, we probed the samples at 4 and 7 days with Oil Red O stain to assess the presence of lipid inclusions. The Oil Red O (ORO) stain was prepared at least 24 hours in advance by adding 0.7 g of Oil Red O powder (Sigma) into 200 ml isopropanol, and mixing that on an orbital shaker overnight. The solution was then filtered through a 0.2 µm filter to remove non-dissolved solute, and diluted down to 60% concentration with 1X PBS.

The cells were fixed with 4% paraformaldehyde (PFA) for 10 minutes at room temperature. The PFA was removed, and the cells washed 3 x 5minutes with 1X PBS. Roughly 2 ml of 60% ORO stain was added to each well, sufficiently covering the gold slide, and placed on the orbital shaker for 45 min at room temperature. Afterwards, the ORO was removed, and the slides were washed 3 x 15minute in 1X PBS prior to imaging on a transmitted light microscope.

4.3 Results

4.3.1 MSC Attachment and Proliferation

Preliminary experiments demonstrated that MSC were capable of adhering and spreading without noticeable morphological differences between

IBDs (data not shown). Figure 4-1 shows that, despite the height of the glass slide, in all conditions cells were able to attach to the modified surface. Despite similar levels of initial attachment, there were differences observed amongst the proliferation profiles. Specifically, FQG demonstrates the slowest proliferation, with a final averaged count of 47,010 cells per slide. TTS demonstrates the most proliferation at day 7, with a final averaged count of 98,371 cells per slide, a greater than 2-fold increase. All other conditions maintained similar growth profiles that was somewhere between these two extremes.

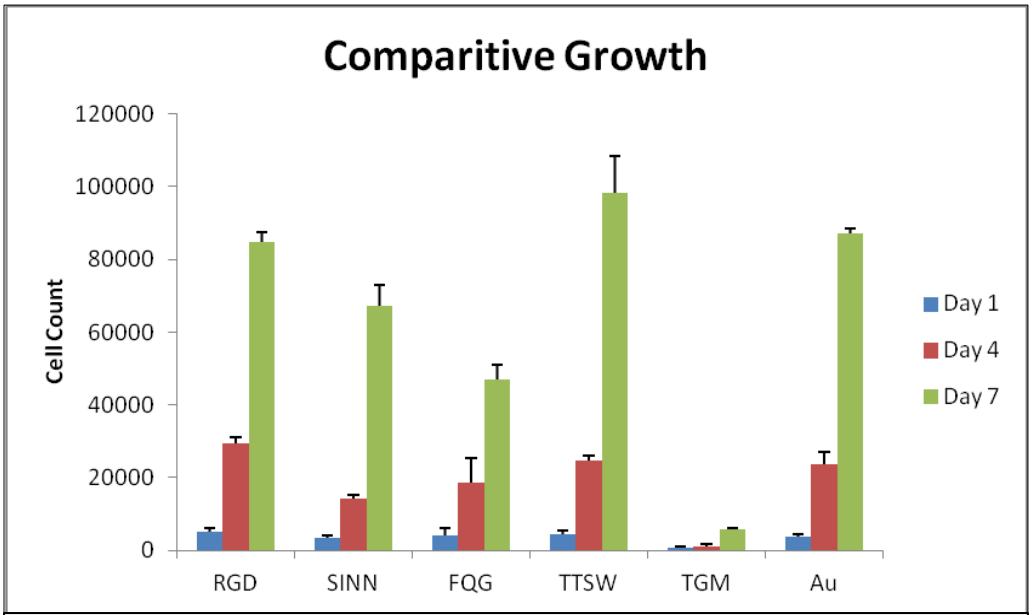

Figure 4-1. MSC attachment to peptide modified gold surfaces and proliferation assessment at 4 and 7 days.

4.3.2 Immunohistology Does Not Demonstrate Cardiogenesis

Figure 4-2 shows representative images from days 1, 4, and 7 (left to right in each series) for each respective peptide. Although nuclei can easily be detected, there is no evidence of localized staining for Nkx2.5 or GATA4 in any condition.

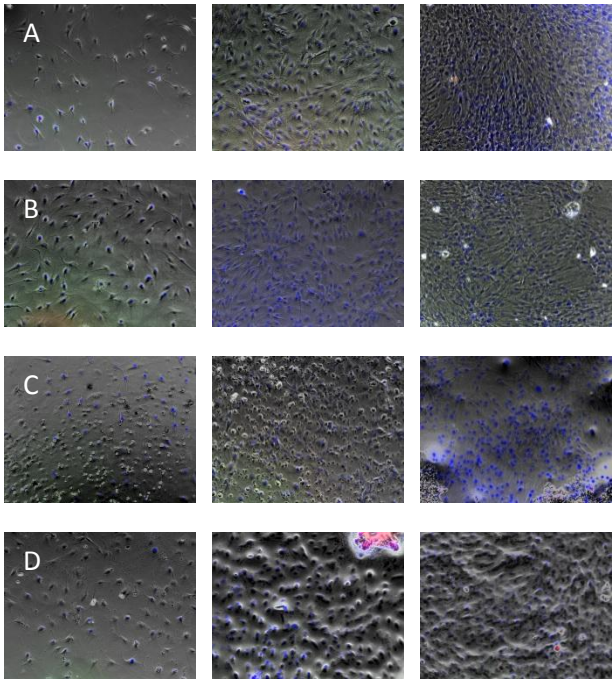

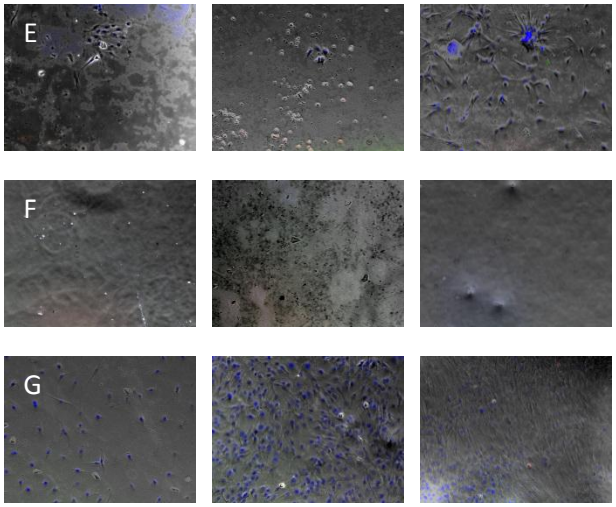

Figure 4-2: Transmitted and fluorescence overlays for day 1, 4, and 7 (left to right) for the seven experiment groups, 10x. (A.) RGD (B.) TTSW (C.) SINN (D.) FQG (E.) TGM (F.) TriG (Negative Control) (G.) Au (Positive Control). Grey- transmitted; Blue- Nuclei; Green- GATA-4; Red- Nkx 2.5

4.3.3 Histology Shows No Evidence of Lipid Inclusion

To assess the possibility of the IBD monolayer to influence MSCs' ability to develop lipid inclusions, Oil Red O was used to stain samples at day 4 (data not shown) and day 7. As can be seen in figure 4-3, there does appear to be a qualitative difference between MSC cultured on IBDs and those cultured on tissue culture plastic.

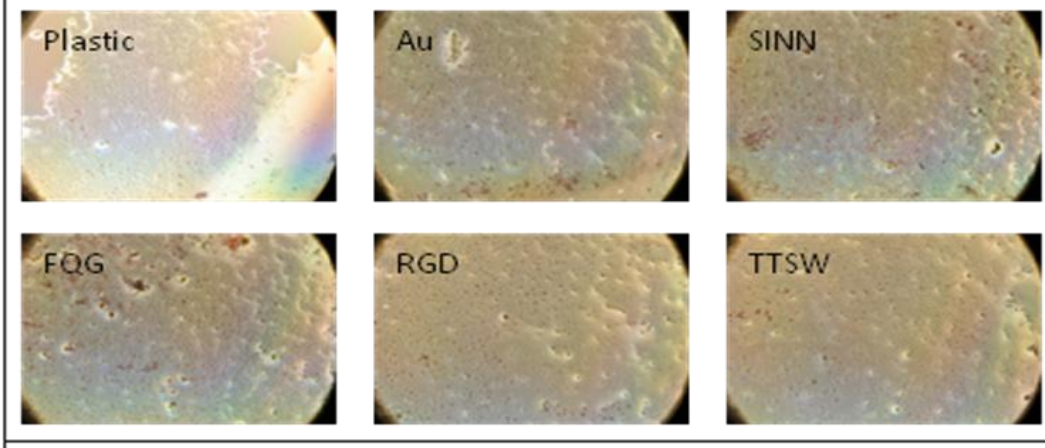

Figure 4-3. Day 7 Oil Red O staining in MSCs cultured on Au, and the peptide monolayers SIN, FQG, RGD, and TTS show no upregulation of lipid inclusion versus the MSCs cultured on tissue culture plastic.

4.4 Discussion

The goal of this study was to explore the ability of thio-linked IBDs to form self-assembled monolayers on a gold surface, and assess their effects on MSC proliferation and differentiation. To investigate this, we reviewed the

literature to identify integrin-binding peptides known to influence cardiac processes during development and remodeling. We then purchased these peptides with the addition of a cysteine residue on the carboxyl end. Gold-sputtering was used to produce a 20 nm gold deposition on glass slides, and these surfaces were functionalized with the purchased peptide monomers. The natural semi-strong thiol-gold bond enabled the monomers to self-assemble into a monolayer, thereby presenting a unified peptide field to the MSCs. We assessed the influence of the IBDs on the proliferation of the MSCs by manually counting random fields-of-view. To evaluate any MSC differentiation response to these culture conditions, we performed immunohistology for markers indicating cardiac differentiation, and Oil Red O staining for lipid inclusion. Our results indicate differences per IBD in proliferation, but not in lipid formation, that suggest this approach to exploring IBD-mediated cell signaling warrants further investigation.

Although studies have demonstrated that proteins can have mitogenic effects on cells, there is a dearth of research exploring how identified integrin-binding sequences might affect cellular behavior. We sought to explore this information gap by assessing how MSCs react to a specific IBD, reasoning that this cell type would be more sensitive to its surroundings than terminally

differentiated cells. The ability to investigate how a cell is capable of transducing information from the surrounding ECM could potentially lead to the determination of a mechanism for integrin-mediated signaling. There are multiple factors that interact as functional determinants of mechanotransductive signaling: tension (133), peptide binding sequences (57), binding synergy sequences (70), and possibly tension-modulated binding activity (89). To better understand these factors in their totality, they must be broken down into their respective components and systematically probed, much as previous work has been done with soluble factor effects on chemotaxis (122), proliferation (64), and differentiation (30).

Gold surfaces modified with the non-binding "peptide" triethylene glycol mono-11 mercaptoundecyl ether (TGMME) inhibited attachment, supporting the fact that the thiol-modified IBDs were capable of developing a self-assembled monolayer that promoted cellular attachment. However, at lower concentrations, the TGMME did allow for some MSC adherence to the surface (Figure 4-2F). This is most likely due to a lack of available TGMME for the available Au-functional sites, thereby allowing cells to adhere directly to the gold as they do in the positive control. Taken together, this implies the possibility that the IBDs might not be achieving 100% coverage, and allowing for some MSCs to

adhere directly to the gold surface. This alternate binding event could ultimately influence the effect of the IBD on a confluent cell sheet by dampening the overall IBD-induced signal or by promoting alternate signaling pathways. Future experiments will account for this by mixing IBDs into a TGMME concentration that has demonstrated 100% inhibition of cellular attachment, thereby ensuring that any attachment, and subsequent effect, can be directly correlated with the peptide of interest.

As seen in the images in Figure 4-2, there is no visible staining for either Nkx2.5 or GATA4, indicating that despite providing a surface attachment, these specific IBDs do not induce a differentiation response when presented individually. A possible explanation for the lack of evidence demonstrating MSC differentiation may be a result of the single IBD presentation. ECM is a dynamic mixture of proteins and polysaccharides that alters in composition over time, influencing the cells even as they remodel it (53, 55, 59). Individual peptides have been shown to influence cell fate, like the use of RGD peptide to increase cellular adhesion (78) and induce vasoconstriction (118), or the use of KRSR to influence osteogenesis (79). However, more complete differentiation has been supported through the use of whole proteins (11), supporting the concept that multiple IBDs influence mitogenic processes (70). Similarly, as evidenced by the

complex results of our PAAm-ECM experiments, the induction of these transcription markers might be tuned to a stiffness that is less than that of glass, concurrent with previous studies linking differentiation to stiffness (11, 15, 17, 22, 23, 75). Furthermore, despite some visible red coloration in Figure 4-3, further investigation revealed that this staining was not localized within the cell as would be expected for lipid inclusions, and is most likely the result of ORO precipitate and not indicative of MSC lipid formation.

These preliminary experiments establish that the thiol-modified IBDs do promote cell adhesion and (in some cases) robust proliferation. Optimizing the platform by suspending the IBD of interest within the non-binding TGMME (to ensure that determined effects can be directly linked to the known IBD) could potentially allow investigations into intracellular signaling regulation and phenotypic response. Once it is further established, this system is readily adapted to investigate multiple IBDs presented on the same surface either through mixed-concentration gradients or more complex patterning with a microspotter. The range of thiol-modified proteins and polysaccharides that can be interrogated via this system is limited only by the published data on the binding site sequences (which is currently small). Future experiments will also have to account for the overlap of multiple integrins binding the same IBD (RGD

for example) by potentially by blocking specific integrins with antibodies prior to culture, or utilizing integrin knock-out cell lines.

The ability to isolate peptide fragments of interest and immobilize them onto a surface represents a strong step toward understanding the signaling mechanisms involved with specific integrin binding. Advancing our knowledge of this poorly understood mechanism would have implications ranging from a better understanding of tissue development and maturation to designing better *in vitro* platforms for experimentation and therapeutic applications.

5. Investigation of Alternate Methods for Extracellular Matrix Solubilization and Hydrogel Casting

5.1 Introduction

Significant attention is being paid to utilizing decellularized ECM as a scaffold for directing MSC differentiation (16, 22-24, 123, 124, 130). The merits of this platform are that it maintains the spatial geometries and microstructure of the organ (16), and contains the total protein component for binding-mediated signaling. However, in practice it has been shown that reseeding total ECM with cells occurs at a low efficiency, inhibiting the cells' ability to adhere and proliferate into the matrix and thus recapitulate normal organ function (16). Given this difficulty, we sought to produce hydrogels solely from solubilized ECM, thereby conserving the de facto composition of the local environment and its important signaling mechanisms.

Hydrogels are widely used as two dimensional and three dimensional platforms for cell culture (26, 113). Current practice generally rely on a common gel "backbone" such as fibrin (126), or polyethylene glycol (PEG) (125), which is then functionalized with growth factors (127), increased or decreased cross-links for influencing motility and hydrogel stiffness (126), and binding domains to

promote cellular attachment (125). These are used individually or in concert to recapitulate the *in vivo* environment and drive a cellular response toward a desired outcome (127).

Previous work has demonstrated that cellular response to stimuli varies between two- and three-dimensional culture, attributed to the fact that cells *in vivo* reside within a flexible three-dimensional space that is unlike the rigid two-dimensional culture conditions on glass or plastic (144). These environmental conditions are sensed via mechanotransduction by the integrins, heterodimeric transmembrane proteins that convey information in a bi-directional manner (76). It has been demonstrated that integrin adhesions, and focal-adhesion kinase activity, are altered when cells are cultured in three-dimensions (146), and that this signal transduction takes on *in vivo* physiological relevance when cells are within a three-dimensional scaffold (145).

Extracellular matrix is commonly solubilized by a method developed in the Badylak lab. Solubilization of some tissue, including small intestine sub-mucosa (124) and pericardium (123), has demonstrated the ability to spontaneously re-assemble when resuspended in biologically relevant pH, tonicity, and salinity. This appears to be a function of collagen I spontaneous re-

assembly that occurs under similar conditions. Unfortunately current methods for solubilizing cardiac ECM, such as those utilized by the Christman lab, have only demonstrated success at re-assembly of cardiac ECM *in vivo* (130). In our own studies, cardiac ECM appears unable to produce a cardiac ECM-based hydrogel *in vitro* that is more than a loose association of precipitate. In this work, we hypothesized that by altering the solubilization protocol, we would be able to preserve innate protein structure and function that would promote the formation of an ECM hydrogel *in vitro*.

In parallel with exploring new methods for solubilizing the ECM, we also sought to explore possible methods for reforming cross-links to promote re-assembly. Ideally, the method by which this is achieved should allow the user to exercise control over the amount of cross-linking, thereby enabling tuning over the hydrogel end-point stiffness. We also hypothesized that utilization of commonly used cross-linking agents would chemically regulate the creation of a hydrogel from the current solubilization protocol.

5.2 Methods

5.2.1 Tissue Decellularization

Lean bovine skeletal muscle was purchased from a local butcher and sliced into thin strips (<0.5 cm) prior to being decellularized by agitation in 1% SDS as described elsewhere in this thesis. Once no visible cellular material remained (approximately 3 days), the ECM was rinsed for several days in 1 liter of 1X PBS that was changed every 12 hours. The ECM was then cut into smaller sections, and squeezed dry with Kimwipes for weighing and approximation of "dry" weight.

Solubilizing Agents

The ECM pieces were resuspended in [a minimum of] 5% w/v in either of the chaotropic agents 8M urea or 9.3M LiBr, respectively, and set on a stirplate at 60°C for observations.

Cross-linking via Gluteraldehyde or N-hydroxysuccinimide

Two alternative methods for creating cross-links were explored:

treatment of the solubilized ECM with gluteraldehyde and N-hydroxysuccinimide. Gluteraldehyde was chosen because it is commonly used to fix tissue samples for imaging via electron microscopy. It denatures alpha-helices, and forms covalent bonds (via methylene bridges) between accessible nitrogen atoms in polypeptide chains (lysine is preferred). N-hydroxysuccinimide is capable of forming covalent bonds between free amine groups and amine-carboxyl groups (as described above).

5.3 Results

5.3.1 Chaotropic Agents are Insufficient to Solubilize ECM

No visible increase in solubilization occurred at 60°C over 3 days for treatment with neither 9.3M LiBr nor 8M Urea. Additional experiments were conducted at 80°C and 100°C with similar results. Applying 120°C degrees to the solution did result in the formation of floating red droplets in the 8M urea (Figure 5-1A), which were lipid-like in appearance. In both solutions at 120°C, the ECM appeared to become less organized, but this was primarily at the edges of the tissue section and was most likely the result of the combination of heat and

mechanical disruption caused by the stirbar (Figure 5-1B).

In one attempt, a 9.3M solution at 140°C appeared to become mostly cloudy as the result of dissociation of the tissue. Unfortunately attempts to dialyze this solution resulted in minor precipitation crash-out (Figure 5-1C), and subsequent dehydration of the concentrated solution failed to produce an ECM construct similar to those seen formed by the same process with silk.

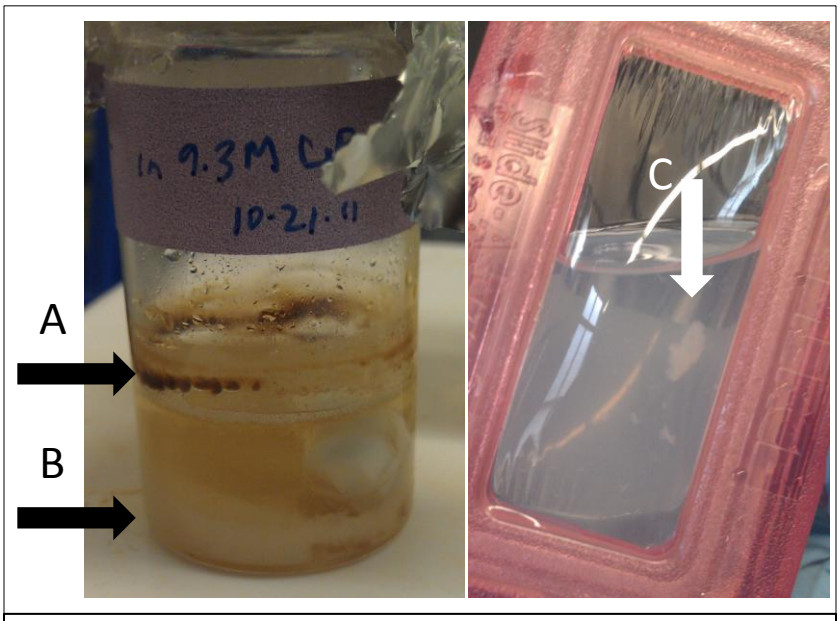

Figure 5-1. Shows representative images depicting the accumulation of floating red "lipid" like solution (A) and non-solubilized ECM (B) in 9.3M LiBr at 120°C. Some solubilized ECM partially crashed out of solution (C, white arrow), but was unrecoverable.

5.3.2 Gluteraldehyde and NHS Treatment Do Not Produce an ECM Hydrogel

Our results show that only at very high concentration was gluteraldehyde capable of producing a droplet of pepsin-digested ECM that appeared to have increased surface tension (Figure 5-2). However, even this increase did not result in a hydrogel that was capable of being manipulated; it was considerably less workable than a polyacrylamide, polydimethyl sulfate, or fibrin based gel.

Figure 5-2. Representative image showing viscous surface tension of solubilized ECM by treatment with high-concentrations of gluteraldehyde

5.4 Discussion

The goal of these experiments was to solubilize decellularized ECM via less harsh methods than currently used. Pepsin is one of the three principal digestive enzymes found within the human stomach. Most active in 0.1M HCl (pH around 1), it is an extremely efficient and indiscriminate protease that cleaves peptide sequences on the amide side of a hydrophobic, aromatic ring containing amino acid (tryptophan, tyrosine, and phenylalanine) (128). Although this makes it ideal for digesting large polypeptides quickly, it is possible that segments of the protein are being over-digested. Over-digestion might result in

the generation of very small peptide fragments that contain only single cross-linking residues. If this were the case, cross-linking would be unable to polymerize chains and/or branched structures necessary for developing a protein mesh. Furthermore, the inherent variability of the digestion (due to even minor variance in temperature, concentrations, etc) causes a lack of control in the downstream output.

An alternate method for solubilizing protein is utilized by the Kaplan lab and others for silk processing. Silkworm silk is composed of 2 proteins: an outer "sticky" layer of sericin and an inner structural protein called fibroin. To process silk, the sericin must be removed prior to the use of lithium bromide (LiBr) to solubilize the fibroin (129). LiBr is able to solubilize the beta-sheet protein because it is a strong chaotropic agent. Chaotropic agents are substances that interrupt the non-covalent interactions between proteins resulting in their dissociation. Other examples of chaotropic agents include urea, guanadinium chloride, ethanol, and phenol.

From these preliminary results, it appears that solubilizing the ECM via chaotropic agents alone is unlikely to achieve total protein dissociation. This is almost certainly attributable to the presence of covalent bonds amongst the

ECM proteins (52, 99, 100, 101); chaotropic agents are incapable of reducing these bonds, and therefore cannot disrupt the protein-protein binding that forms a critical component to maintaining the underlying stiffness (96). Although fibroin's quaternary structure can undergo chaotropic disruption (129), sodium dodecyl sulfate is itself a chaotropic agent and is used to remove cellular material from the tissue with minimal collateral damage to the ECM. Removal or reduction of protein cross-links will most likely have to be achieved by alternate methods, possibly via reduction of the disulfide bonds with either 2-mercaptoethanol or tris(2-carboxyethyl)phosphine (TCEP).

Furthermore, our observations in attempting to chemically cross-link protein solubilized by standard methods lend some support to the hypothesis that pepsin does cause over-digestion that can result in very small protein fragments incapable of supporting large polymerization. In order to build a hydrogel mesh, the majority of peptide fragments would need to contain at least two attachment points. The very small fragments that could be here would act as terminal end-points along a propagation, the result of which would be aggregated protein strings, not a true interconnected mesh. If sufficiently large polypeptides were present (each containing multiple binding sites), a protein mesh should form in the presence of increasing concentrations of these cross-

linking agents. At the highest concentration, gluteraldehyde was observed to increased surface tension (data not shown), but this did not result in a true hydrogel. None of the samples produced a gel that approached the form, shape, or stiffness of the ECM in its natural state. Despite achievements in re-assembly of the solubilized cardiac ECM *in vivo* (130), our own attempts have yet to yield a hydrogel on the bench top. At best, our attempts – following published protocols – yield an extremely soft and loose aggregation. Although it is theoretically possible to increase the gluteraldehyde concentration further, the highest concentration we tested is concurrent with other products approved for human use (131). Going beyond this limit might obviate the applicability of an ECM-based hydrogel. Future work should examine the efficacy of denaturing disulfide bonds (as mentioned above) prior to chaotropic treatment, and explore the use of other [or a mixture of] cross-linking agents that have various binding targets. The ability to form a hydrogel from native ECM has broad-spectrum potential, and despite the hurdles encountered during these preliminary investigations, further work exploring this potential is warranted.

6. Summary

As cell-based therapy approaches have gained popularity for addressing challenges in regenerative medicine, increased attention is being directed toward developing patient-specific cells *in vitro* to obviate immune complications *in vivo*. Three types of proliferating multipotent cell populations have been the subject of considerable research: embryonic stem cells (ESC), induced pluripotent stem cells (iPSC), and mesenchymal stem cells. Each platform has its own strengths and weaknesses. ESCs by nature are totipotent, and have been shown to generate cardiomyogenic like cells *in vitro* (27, 29, 30). Ultimately, however, their use is limited by primary cell isolation and immune complications common to allogenic material (31). iPSCs are dedifferentiated autologous pluripotent cells, theoretically removing the bottleneck of cell supply. Unfortunately recent data indicates that the current dedifferentiation process can induce a host immune response, resulting in the likelihood for the need of immunosuppressants and/or increased incidence of teratocarcinoma (35, 36). MSC are a pluripotent, proliferating, patient-specific cell source that naturally regenerates within the body and can be expanded *in vitro* to clinically relevant numbers (37). They have been shown to generate cardiomyogenic cells *in vitro*, but current methods demonstrate low differentiation efficiency (27, 66).

The extracellular matrix provides a support structure for cell proliferation and function. Previously this structure was thought to be passive, however it is quickly becoming realized as an important signaling molecule to cells (55). Evidenced by the variety of downstream interactions integrin binding events have on key intracellular signaling pathways, it seems apparent that local environmental cues can dramatically influence cell behavior (85-88). Although it's been known for years that cells will migrate to tissue appropriate stiffness during mechanotaxis (69), only recently has it been demonstrated that pluripotent stem cells will mechanodifferentiate in a similar manner (15). Singular protein presentation might demonstrate an increased proliferation on collagen I (139), or an increased cell adhesion, but decreased proliferation, on fibronectin (81), but these studies fail to explain how the binding to these two proteins at the same time might synergistically or antagonistically affect the cell. Furthermore, while decellularized ECM has been shown to support cardiomyocyte function (23, 24), and substrate stiffness has been identified as important for cell function (15, 133), there is minimal published data exploring the combination of these factors and their potential role on MSC cardiac differentiation.

One distinct advantage of our approach is the recapitulation of this

binding site complexity. Providing the complex ECM protein mixture in this fashion consistently demonstrated that total [neonatal] ECM presentation had the greatest propensity for inducing cardiac differentiation. While a lack of confidence in the ELISA data prevents a mechanistic correlation to the binding profile that might be responsible for the observed results, it does not disqualify them. Moreover, when this result is taken with the IBD results in Chapter 4, it appears that total ECM is more capable of promoting differentiation than its individual parts (see Figure 3-6 vs 4-2). However, as the experiments in Chapter 4 were preliminary, a more thorough examination of the IBDs is warranted as discussed below.

Although this platform has been developed as proof-of-concept, it definitively shows that there are complex relationships governing gene activation and protein translation as a function of substrate stiffness and composition. From the data shown in this thesis we might be able to hypothesize that stiffness modulated tension and integrin binding events transduce signal across the cell membrane by separate but interdependent pathways, and that these pathways most likely interact to control mitogenic processes. Future experiments could attempt to probe this by utilizing ligands known to inhibit particular pathways involved in differentiation and mechanotransduction, such

as the Rho/ROCK inhibitor Y27632 (76). Alternatively, integrin-knockout cell lines could be established to probe individual contribution to cell fate, as suggested by previous work (145).

It is important to note the challenges that this platform presents. Considerable effort was dedicated to troubleshooting protocols that were adapted for Western blotting. Early attempts to isolate protein and mRNA from the PAAm-ECM without trypsanization yielded no product. Investigations revealed the most likely cause to be a natural affinity of proteins to polyacrylamide, inhibiting any possible recovery (116). Trypsanization of the cells prior to sonication yielded modest, albeit usable, results for Western blotting. However, successful QPCR has yet to be achieved. Imaging through the thin PAAm-ECM layer doesn't pose a problem at 10x magnification, but the inherent protein affinity of the polyacrylamide causes the PAAm to collect a high fluorescently-labeled antibody background that can cause difficulty for automated cell delineation. Ultimately a global pipeline was developed in CellProfiler that removed the background, but we potentially lost sensitivity of the measurement as a result. Continued efforts to optimize these quantitative assays are warranted to increase the efficacy of this platform.

7. Conclusions Future Directions

7.1 PAAm-ECM

As with any new platform, there are many avenues for improvement and application, and identifying potential improvements is part of the development process. It appears that the cells are detaching from the PAAm-ECM as early as 2 weeks. This is most likely due to the inability of the cells to remodel the surface with new ECM because the PAAm lacks functional groups to anchor them (76, 116). Potentially this could be overcome by producing a modified backbone unit composed of a non-binding peptide sequence. Introducing amino acids into the backbone of the gel could produce attachment sites for newly synthesized proteins without influencing the self-assembly of the polyacrylamide, thereby maintaining the ability to tune the stiffness. Although functionalizing a self-assembling protein (like collagen I) might be attractive, using a peptide with binding domains might have undue consequences on signaling. It would likely be better to modify an inert backbone and limit adding more variables into the equation, thereby limiting any of the undue effects of using a peptide with binding sites.

It would also be very useful to know what happens to cells that have been pre-differentiated in this culture system when applied to other applications. Going forward, it would be interesting to see if MSCs that have been activated by this platform display an increased propensity to become mature, contractile, cardiomyocytes in the presence of soluble factors, and mechanical and/or electrical stimulation, as has been previously demonstrated (148). Following that, incorporating those additional stimuli directly into this platform would further recapitulate the *in vivo* environment, and may lead to the development of contracting cardiomyocytes without soluble factors.

Perhaps the most interesting part of this work is the implication that adult stem cells can be driven toward a desired phenotype by culturing them on a complex mixture of ECM proteins. As evidenced by the lack of observed signal when the MSCs were cultured on individual proteins at various stiffnesses, it appears that the complex combination of proteins that form the ECM are required to promote directed differentiation. It will be interesting to examine whether transdifferentiation of cardiac fibroblasts (and other accessory cells) might be possible via this approach. Additionally it might be possible to derive disease-specific and/or organ-specific protein ratios via proteomic methods (peptide fingerprinting, etc), and then use off-the-shelf purified proteins to

enhance current *in vitro* platforms.

7.2 IBD Binding

Although the IBD binding did not induce any interrogated effect, it is still a justified platform for interrogating signaling via a specific integrin heterodimer. The ability to isolate peptide fragments of interest and immobilize them onto a surface represents a strong step toward understanding the signaling mechanisms involved with specific integrin binding. Furthermore, this platform allows the user to rapidly interrogate the effects of multiple integrins deposited on the surface, and easily change their respective ratios without the use of specialized equipment.

Going forward with this platform, the next set of experiments should determine the concentration of blocking peptide needed to ensure complete inhibition of cell-gold binding. After that, these experiments should be re-run to validate the cell response and determine a working range for IBDs to be presented to the cell that encourage “normal” adhesion and proliferation. Following that, a combinatorial study of the current IBDs should be undertaken,

while simultaneously repeating the process with newly identified IBDs. Comprehensive analysis of the genetic effects these binding events have might best be elucidated by running geneChips, otherwise it might be useful to explore transforming a cell line to report various changes along the mitogenic pathways.

7.3 ECM Hydrogel

This process appears to have the steepest uphill. It is not clear that there exists a cost-effective, high-throughput way to dissociate tissues in an organized fashion. Possibly there are bacteria or mammalian cells that can accomplish this that have not been previously described, but this seems unlikely. Trying to marry the two processes directly is also a non-starter: chaotropic agents will denature pepsin. It might be possible to start the digestion with pepsin and switch to a chaotropic, but this wouldn't necessarily decrease the likelihood of very small peptide fragments which might prevent the hydrogel mesh from forming.

Looking at ways to improve cross-link formation has similar pitfalls. Trying to induce cross-links without using harmful amounts of chemical reagent appears difficult. Part of the problem can be attributed to the loss of tertiary and

quaternary structure during digestion. That said, other labs do claim to have successful gelation *in vivo*; potentially using serum and/or a maintenance cell (fibroblast) might allow reforming of the matrix. However, more likely the immediate answer should be in exploring other cross-linking agents that don't rely on a one-to-one bridge; cross-linking agents that have multiple arms are more likely to build a web regardless of limiting very small fragment dead-ends. Recently, an interesting development has been the recognition that protein cross-linking can result from incubation with various saccharides (147). As saccharides do not pose the same potential harm as some of the chemicals we've described, they might represent a cell-safe alternative for generating ECM hydrogels, and warrant investigation in this system.

8. References

1. Roger et al *Heart Disease and Stroke Statistics – 2011 Update: A Report from the American Heart Association* Circulation 2011, 123:e18-e209

2. Guyton and Hall *Textbook of Medical Physiology, Twelfth Edition* Saunders, 2011

3. Dangas et al *Restenosis: Repeat Narrowing of a Coronary Art : Prevention and Treatment* Circulation, 2002, 105:2586-2587

4. Rodriguez et al *Coronary stenting versus coronary bypass surgery in patients with multiple vessel disease and significant proximal LAD stenosis: results from the ERACI II study* Heart, 2003; 89:184-188

5. Goldman et al *Radial Artery Grafts vs Saphenous Vein Grafts in Coronary Artery Bypass Surgery* JAMA, 2011; 305(2):167-174

6. Michaels et al *Angioplasty Versus Bypass Surgery for Coronary Artery Disease* Circulation, 2003; 106:e187-e190

7. James, Thomas *Sudden Death Related to Myocardial Infarction* Circulation, 1972; XLV:205-216

8. Pinto et al *Electrical remodeling in ischemia and infarction* Cardiovascular Research 42 (1999) 284-297

9. Rubin et al *Compensatory hypertrophy in the heart after myocardial infarction in the rat* Journal o the American College of Cardiology, (1, 6) 1983; 1435-1441

10. Van den Borne et al *Myocardial remodeling after infarction: the role of myofibroblasts* Nature Reviews Cardiology, 2010; 7:30-37

11. Rowlands A S, George P A, Cooper-White J J Directing osteogenic and myogenic differentiation of MSCs: interplay of stiffness and adhesive ligand presentation *Am J Phys Cell Phys* 295: C1037-C1044, 2008

12. Ieda M, Fu J, Delgado-Olguin P, Vedantham V, Hayashi Y, Bruneau B, Srivastava D Direct reprogramming of fibroblasts into functional cardiomyocytes by defined factors *Cell* 142: 375-386, 2010

13. Tan G, Shim W, Gu Y, Qian L, Ying Chun Y, Yun Lim S, Yong P, Sim E, Wong P

Differential effect of myocardial matrix and integrins on cardiac differentiation of human mesenchymal stem cells *Differentiation* 79: 260-271, 2010

14. Kuraitis D, Ruel M, Suuronen E Mesenchymal stem cells for cardiovascular regeneration *Cardiovasc Drugs Ther* v25, 4: 349-362, 2011

15. Engler, A. J., Sen, S., Sweeney, H. L., & Discher, D. E. (2006). Matrix elasticity directs stem cell lineage specification. *Cell*, *126*(4), 677-89. doi:10.1016/j.cell.2006.06.044

16. Ott, H. C., Matthiesen, T. S., Goh, S.-K., Black, L. D., Kren, S. M., Netoff, T. I., & Taylor, D. a. (2008). Perfusion-decellularized matrix: using nature's platform to engineer a bioartificial heart. *Nature medicine*, *14*(2), 213-21. doi:10.1038/nm168

17. Yoon et al *Cell adhesion and detachment on gold surfaces modified with thiol functionalized RGD peptide* Biomaterials, 2011; 32(30):7286-7296

18. Mazuji et al *Siliconized Dacron as a Pericardial Patch* Arch Surg 1963; 87:446-449

19. Rostad et al *Total Correction of Fallot's Tetralogy* Scand J Thor Cardiovasc Surg 1976; 10:131-134

20. Backer et al *Coarctation of the Aorta: Repair with Polytetrafluorethylene Patch Aortoplasty* Circulation, 1995; 92:132-136

21. Stevens et al *Scaffold-free human cardiac tissue patch created from embryonic stem cells* Tissue Eng A, 2009; 15,6:1211-1223

22. Wang et al *Fabrication of Cardiac Patch with Decellularized Porcine Myocardial Scaffold and Bone Marrow Mononuclear Cells* Journal of Biomed Mater Res A, 2010; 94(4):1100-1110

23. Kochupura et al *Tissue-Engineered Myocardial Patch Derived from Extracellular Matrix Provides Regional Mechanical Funtion* Circulation, 2005; 112:144-149

24. Zimmerman et al *Cardiac Grafting of Engineered Heart Tissue in Syngenic Rats* Circulation, 2002; 106:151-158

25. Berry et al *Mesenchymal stem cell injection after myocardial infarction improves myocardial compliance* J Physiol Heart Circ Physiol, 2006; 290:2196-2203

26. Lu et al *Functional Improvement of Infarcted Heart by Co-Injection of Embryonic Stem Cells with Temperature-Responsive Chitosan Hydrogel* Tissue Eng A, 2009; 15(6):1437-1440

27. Malliaras et al *The Stuttering Progress of Cell Therapy for Heart Disease* Nature, 2011; 90(4)532-541

28. Thomson et al *Isolation of a primate embryonic stem cell line* Proc Natl Acad Sci, 1995; 92:7844-7848

29. Murray et al *Differentiation of Embryonic Stem Cells to Clinically Relevant Populations: Lessons from Embryonic Development* Cell, 2008; 132:661-680

30. Takahashi et al *Ascorbic Acid Enhances Differentiation of Embryonic Stem Cells Into Cardiac Myocytes* Circulation, 2003; 107:1912-1916

31. Thomson et al *Embryonic Stem Cell Lines Derived from Human Blastocysts* Science, 1998; 282(5391):1145-1147

32. Takahasi et al *Induction of Pluripotent Stem Cells from Mouse Embryonic and Adult Fibroblast Cultures by Defined Factors* Cell, 2006; 126:663-676

33. Takahasi et al *Induction of Pluripotent Stem Cells from Adult Human Fibroblasts by Defined Factors* Cell, 2007; 131:1-12

34. Ben-David et al *The tumorgenicity of human embryonic and induced pluripotent stem cells* Nature Rev Cancer, 2011; 11:268-277

35. Zhao et al *Immunogenicity of induced pluripotent stem cells* Nature, 2011;474:212-215

36. Apostolou et al *Stem Cells: iPS cells under attack* Nature, 2011; 474:165-166

37. Williams et al *Mesenchymal Stem Cells; Biology, Pathophysiology, Translational Findings, and Therapeutic Implications for Cardiac Disease* Circ Research, 2011; 109:923-940

38. Song et al *Specific differentiation of mesenchymal stem cells by small molecules* Am J Stem Cell, 2012; 1(1):22-30

39. Hwang et al *Chemicals that modulate stem cell differentiation* PNAS, 2008; 105(21)7467-7471

40. Wu et al *Purmorphamine induces osteogenesis by activation of the hedgehog signaling pathway* Chem & Bio, 2004; 11:1229-1238

41. Jaiswal et al *Adult Human Mesenchymal Stem Cell Differentiation to the Osteogenic or Adipogenic Lineage is Regulated by the Mitogen-activated Protein Kinase* J Biological Chem, 1999; 275(13):9645-9652

42. Gang et al *Skeletal Myogenic Differentiation of Mesenchymal Stem Cells Isolated from Human Umbilical Cord Blood* Stem Cells, 2004; 22:617-624

43. Zuk et al *Multilineage cells from Human Adipose Tissue: Implications for Cell Based Therapies* Tissue Eng A, 2001;7(2)211-228

44. Pittenger et al *Multilineage potential of adult human mesenchymal stem cells* Science, 1999; 284:143-147

45. Huang et al *Differentiation of Allogeneic Mesenchymal Stem Cells Induces Immunogenicity and Limits Their Long-Term Benefits for Myocardial Repair* Circulation, 2010;122:2419-2429

46. Solmesky et al *Serum Free Cultured Bone Marrow Mesenchymal Stem Cells as a Platform to Characterize the Effects of Specific Molecules* PLoS One, 2010;5(9):e12689

47. Hass et al *Different populations and sources of human mesenchymal stem cells (MSC): a comparison of adult and neonatal tissue-derived MSC* Cell Commun Signal, 2011; 9:12

48. Caplan, AI *Adult Mesenchymal Stem Cells for Tissue Engineering Versus Regenerative Medicine* J Cell Physiol, 2007; 213:341-347

49. Yoon et al *Transdifferentiation of mesenchymal stem cells into cardiomyocytes by direct cell-to-cell contact with neonatal cardiomyocytes but not adult cardiomyocytes* Ann Hematol, 2005; 84:715-721

50. Takeda et al *Can the life span of human marrow stromal cells be prolonged by bmi-1, E6, E7, and/or telomerase without affecting cardiomyogenic differentiation?* J Gene Med, 2004; 6:833-845

51. Alberts et al *Molecular Biology of the Cell, 4th Edition* Garland Science, 2002

52. Kielty et al *Elastic Fibres* J Cell Science, 2002; 115:2617-2828

53. Colognato et al *Form and Function: the Laminin Family of Heterotrimers* Developmental Dynamics, 2000; 218:213-234

54. Rodin et al *Long-term self-renewal of human pluripotent stem cells on human recombinant laminin-511* Nature Biotech, 2010; 28:611-615

55. Bowers et al *The extracellular matrix: at the center of it all* J Mol and Cell Cardiology, 2010; 48:474-482

56. Pflieger et al *Comparative proteomic analysis of extracellular proteins secreted by two types of skin fibroblasts* Proteomics, 2006; 6:5868-5879

57. Tulla et al *Selective binding of collagen by integrin a1I, a2I, and a10I domains* J Biol Chemistry, 2001; 276(51):48206-48212

58. Pankov et al *Fibronectin at a glance* J Cell Science, 2002; 115:3861-3863

59. Grinnel, Frederick *Fribronectin and wound healing* J Cell Biochemistry, 1984; 26:107-116

60. Toma et al *Human mesenchymal stem cell differentiate to a cardiomyocyte phenotype in the adult murine heart* Circulation, 2002; 105:93-98

61. Yoon et al *Differentiation, engraftment, and the functional effects of a pre-treated mesenchymal stem cells in a rat myocardial infarct model* Acta Cardiology, 2005; 60:277-284

62. Xie et al *Differentiation of bone marrow mesenchymal stem cells induced by myocardial medium uner hypoxic conditions* Acta Pharma Sin, 2006; 27: 1153-1158

63. Hanh et al *Pre-treatment of mesenchymal stem cells with a combination of growth factors enhances gap junction formation, cytoprotective effect on cardiomyocytes, and therapeutic efficacy for myocardial infarction* J Amer Coll Cardiol, 2008; 51(9):933-934

64. Forte et al *Hepatocyte growth factor effects on mesenchymal stem cells: proliferation, migration, and differentiation* Stem Cells, 2006; 24:23-33

65. Nesselman et al *Mesenchymal stem cells and cardiac repair* J Cell Mol Med, 2008; 12(5B):1795-1810

66. Martin-Rendon et al *Azacytidine-treated human mesenchymal stem/progenitor cells derived from umbilical cord, cord blood, and bone marrow do not generate cardiomyocytes in vitro at high frequencies* Vox Sang, 2008; 95:137-148

67. Hou et al *Radiolabeled cell distribution after intramyocardial, intracoronary, and interstitial retrograde coronary venous delivery: implications for current clinical trials* Circulation, 2005; 112:1150-1156

68. Terrovitis et al *Noninvasice quantification and optimization of acute cell retention by in vivo positron emission tomography after the intramyocardial cardiac-derived stem cell delivery* J Am Coll Cardiol, 2009; 54:1619-1626

69. Schwarts, MA *Integrins and extracellular matrix in mechanotransduction* Cold Psring Harb Perspect Biol, 2010; 2:a005066

70. Friedland et al *Mechanically activated integrin switch controls a5b1 function* Science, 2009; 323:642-645

71. Wang et al *Substrate stiffness regulates the proliferation, migration, and differentiation of epidermal cells* Burns, 2011; 3601

72. Provenzano et al *Mechanical signaling through the cytoskeleton regulates cell proliferation by coordinated focal adhesion and Rho GTPase signaling* J Cell Science, 2011; 124(23):1195-1205

73. Evans et al *Substrate stiffness affects early differentiation events in embryonic stem cells* European Cells and Materials, 2009; 18:1-14

74. Hu et al *The influence of elasticity and surface roughness on myogenic and osteogenic differentiation of cells on silk-elastin biomaterials* Biomaterials, 2011; 32(34):8979-8989

75. Tse et al *Stiffness gradients mimicking in vivo tissue variations regulate mesenchymal stem cell fate* PLoS One, 2010; 6(1):e15978

76. Holle et al *More than a feeling: discovering, understanding, and influencing mechanosensing pathways* Curr Op in Biotechnology, 2011; 22:648-654

77. Murphy et al *Nanoparticle-mediated drug deliver to tumor vasculature suppresses metastasis* PNAS, 2008; 105(27): 9343-9348

78. Ruoslahti E. *RGD and other recognition sequences for integrins*. Annu Rev Cell

Dev Biol 1996;12:697–715

79. Schuler et al *Comparison of the response of cultured osteoblasts and osteoblast outgrown from rat calvarial bone chips to nonfouling krsr and fhrrika-peptide modified rough titanium surfaces* J Biomed Material Res B, 2009; 91B(2):517-527

80. Garcia et al *Bio-adhesive surfaces to promote osteoblast differentiation and bone formation* J Dental Res, 2005; 84(5):407-413

81. Balcells et al *Effect of pre-adsorbed proteins on attachment, proliferation, and functionof endothelial cells* J Cell Phys, 2002; 191(2)155-161

82. Cheng et al *Fabricating autologous tisse to engineer artificial nerve* Microsurgery, 2002;22:133-137

83. Sniadecki et al *Microfabricated silicone elastomeric post arrays for measuring traction forces of adherent cells* Methods in Cell Biology, 2007; 83:313-328

84. Quint et al *Decellularized tissue-engineered blood vessel as an arterial conduit* PNAS, 2011; 108(22);9214-9219

85. Ramachandran et al *Rho-Rho kinase pathway in the actomyosin contraction and cell-matrix adhesion in immortalized human trabecular meshwork cells* Molecular Vision, 2011;17:1877-1890

86. Mruthyunjaya et al *Laminin-1 induces neurite outgrowth in human mesenchymal stem cells in serum/differentiation factors-free conditions through activation of FAK-MEK/ERK signaling pathways* Biochem and Biophys Res Comm, 2010; 391:43-48

87. Lee et al *Nobiletin, a citrus falvonoid, suppresses invasion and migration involving FAK/PI3K/Akt and small GTPase signals in human gastric adenocarcinoma in AGS cells* Mol Cell Biochem, 2011;347:103-115

88. Wade et al *Paxillin enables attachment-indpendent tyrosine and phosphorylation of focal adhesion kinase and transformation by ras* J Biol Chem, 2011;286:37932-37944

89. Grashoff et al *Measuring mechanical tension across vinculin reveals regulation of focal adhesion dynamics* Nature, 2011; 466(7303):263-266

90. Kanchanawong et al *Nanoscale architecture of intergrin-based cell adhesions* Nature, 2010; 468(25):580-586

91. Laser et al *Integrin activation and focal complex formation in cardiac hypertrophy* J Biol Chem, 2000;275(48):35624-35630

92. Choi et al *Mechanical derivation of functional myotubes from adipose-derived stem cells* Biomaterials, 2011;epub:1-10

93. Sutton et al *Left Ventricular Remodeling After Myocardial Infarction: Pathophysiology and Therapy* Circulation, 2000;101:2981-2988

94. Wernig et al *In vitro reprogramming of fibroblasts into a pluripotent ES-cell-like state* Nature, 2007;448:318-324

95. Kadler et al *Collagen fibrillogenesis: fibronectin, integrins, and minor collagens as organizers and nucleators* Cur Opin Cell Bio, 2008;20(5-24):495-501

96. Lullo et al *Mapping the ligand-binding sites and disease-associated mutations on the most abundant protein in the human, type I collagen* J Biol Chem, 2002;277(6):4223-4231

97. Liu et al *Type III collagen is crucial for collagen I fibrillogenesis and for normal cardiovascular development* PNAS, 1997; 94(5):1852-1856

98. Mendler et al *Cartilage contains mixed fibrils of collagen types II, IX, and XI* J Cell Bio, 1989; 108:191-197

99. Laurie et al *Localization of type IV collagen, laminin, heparin sulfate proteoglycans, and fibronectin to the basal lamina of basement membranes* J Cell Bio , 1982;95(1)340-344

100. Wenstrup et al *Type V collagen controls the initiation of collagen fibril assembly* J Biol Chem, 2004;279(51):53331-53337

101. Mao et al *Fibronectin fibrillogenesis, a cell-mediated matrix assembly process* Matrix Biology, 2005; 24:389-399

102. Hynes et al *The extracellular matrix: not just pretty fibrils* Science, 2009;326:1216-1222

103. Eikelenboom et al *Cellular and substrate adhesion molecules (integrins) and*

their ligands in cerebral amyloid plaques in Alzheimer's disease Virchows Archiv, 1994; 424:421-427

104. Giancotti et al *Integrin Signaling* Science, 1999;285:1028-1032

105. Solovjov et al *Distinct roles for the a and b subunits in the functions of integrin aMb2* J Biol Chem, 2005;280(2):1336-1345

106. Durocher et al *The cardiac transcription factors Nkx2.5 and GATA4 are mutual cofactors* EMBO, 1997;16(18):5687-5696

107. Young et al *Human cardiomyogenesis and the need for systems biology analysis* Wiley Interdiscip Rev Syst Biol Med, 2011;3(6):666-680

108. Akazawa et al *Cardiac transcription factor Csx/Nkx2-5: Its role in cardiac development and diseases* Pharm & Therapeutics, 2005;107:252-268

109. Karamboulas et al *Disruption of MEF2 activity HDAC in cardiomyoblasts inhibits cardiomyogenesis* J Cell Science, 2006; 119:4315-4321

110. Dodou et al *Mef2C is a direct transcriptional target of ISL1 and GATA factors in the anterior heart field during mouse embryonic development* Development, 2004;131:3931-3942

111. Ieda et al *Direct Reprogramming of Fibroblasts into Functional Cardiomyocytes by Defined Factors* Cell, 2010;142:375-386

112. Reinecke et al *Skeletal muscle stem cells do not transdifferentiate into cardiomyocytes after cardiac grafting* J Mol Cell Cardiol, 2002; 34(2):241-9

113. Ye et al *Encapsulation of cardiomyocytes in a fibrin hydrogel for cardiac tissue engineering* J Vis Exp, 2011;55:e3251

114. Safety Study of GRNOPC1 in Spinal Cord Injury, http://clinicaltrials.gov/ct2/results?term=NCT01217008

115. Black, LD *Mechanical and failure properties of lung and engineered tissues as a function of structural protein composition* Boston University, 2006

116. Sazonova et al *Cell-cell interactions mediate the response of vascular smooth muscle cells to substrate stiffness* Biophysical Journal, 2011;101:622-630

117. Nadruz et al *Focal adhesion kinase mediates MEF2 and c-Jun activation by stretch: Role in the activation of the cardiac hypertrophic genetic program* Cardiovasc Res, 2005;68(1)87-97

118. Mogford, J.E., G.E. Davis, and G.A. Meininger, *RGDN peptide interaction with endothelial alpha5beta1 integrin causes sustained endothelin-dependent vasoconstriction of rat skeletal muscle arterioles.* J Clin Invest, 1997. 100(6): 1647-53.

119. Collo, G., et al., *Gradient of integrin alpha 6A distribution in the myocardium during early heart development.* Cell Adhes Commun, 1995. 3(2):101-13.

120. Maitra, N., et al., *Expression of alpha and beta integrins during terminal differentiation of cardiomyocytes.* Cardiovasc Res, 2000. 47(4):715-25.

121. Matter, M.L. and G.W. Laurie, *A novel laminin E8 cell adhesion site required for lung alveolar formation in vitro.* J Cell Biol, 1994. 124(6):1083-90

122. Amadi et al *A low resistance microfluidic system for the creation of stable concentration gradients in a defined 3D microenvironment* Biomed Microdevices, 2010; 12(6):1027-1041
123. Wainwright et al *Preparation of Cardiac Extracellular Matrix from an Intact Porcine Heart* Tissue Eng A, 2010; 16(3):525-532
124. Badylak et al *Extracellular matrix for myocardial repair* Heart Surg Forum, 2003;6(2):E20-26
125. Kraehenbuehl et al *Three-dimensional extracellular matrix-directed cardioprogenitor differentiation: systemic modulation of a synthetic cell-responsive PEG-hydrogel* Biomaterials, 2008;29:2757-2766
126. Yuan et al *Encapsulation of cardiomyocytes in a fibrin hydrogel for cardiac tissue engineering* J Vis Exp, 2011;55:3251
127. DeLong et al *Covalently immobilized gradients of bFGF on hydrogel scaffolds for directed cell migration* Biomaterials, 2005;26(16):3227-323
128. Dunn et al *Overview of pepsin-life aspartic peptidases* Curr Protoc Protein Sci, 2001;Chapter 21
129. Rockwood et al *Materials fabrication from Bombyx mori silk fibroin* Nat Protoc, 2011;6(10):1612-1631
130. Singelyn et al *Naturally derived myocardial matrix as an injectable scaffold for cardiac tissue engineering* Biomaterials, 2009;30:5409-5416
131. Umashankar et al *Short duration gluteraldehyde cross linking of decellularized bovine pericardium improves biological response* J Biomed Mater Res A, 2011;97(3):311-320

132. Kuhn et al *Periostin induces proliferation of differentiated cardiomyocytes and promotes cardiac repair* Nat Med, 2007;13(8)962-969
133. Engler et al *Substrate Compliance versus Ligand Density in Cell on Gel Responses* Biophysical Journal, 2004;86:617-628
134. Wood et al *Wound healing recapitulates morphogenesis in Drosphilia embryos* Nature Cell Bio, 2002;4:907-912
135. Black et al *Effects of elastase on the mechanical and failure properties of engineered elastin rich matrices* J Appl Physiol, 2005;98(4)1434-1441
136. Lammerding et al *Mechanotransduction in cardiac myocytes* Annual N Y Acad Sci, 2004;1015:53-70
137. Arminin et al *Cardiac differentiation is driven by Nkx2.5 and Gata4 nuclear translocation in tisse-specific mesenchymal stem cells* Stem Cells and Dev, 2009;18:907-918
138. Lahiri et al *Patterning ligands on reactive SAMs by microcontact printing* Langmuir, 1999;15(6):2055-2060
139. Celebi et al *Effects of extracellular matrix proteins on the growth of hematopoietic progenitor cells* Biomed Mater, 2011;6:055011
140. Camarata et al *LMP4 regulates Tbx5 protein subcellular localization and activity* J Cell Bio, 2006; 174(3):339-348
141. Jacot et al *Cardiac myocytes force development during differentiation and maturation* Annal NY Acad Sci, 2010;1188:121-127
142. Maitra et al *Expression of alpha and beta integrins during terminal differentiation of cardiomyocytes* Cardiovasc Res, 2000;47(4):715-725
143. Le Guillor-Buffello et al *Additive effect of RGD coating to functionalized titanium surfaces on human osteoprogenitor adhesion and spreading* Tisse Eng Part A, 2008;14(8):1445-1455
144. Esldale et al *Collagen substrata for studies on cell behavior* J Cell Bio, 1972;54:626-637
145. Cukierman et al *Cell interactions with three-dimensional matrices* Curr Opin Cell Bio, 2002;14(5):633-640
146. Cukierman et al *Taking cell-matrix adhesions to the third dimension* Science, 2001;294:1708-1793
147. Ter Haar et al *Cross-linking behavior and foaming properties of bovine α-lactalbuminafter glycation with various saccharides* J Agric Food Chem, 2011;59(23)12460-12466
148. Guan et al *The stimulation of the cardiac differentiation of mesenchymal stem cells in tissue constructs that mimic myocardium structure and biomechanics* Biomaterials, 2011;32(24):5568-5580